NASA Contractor Report 202350

An Efficient Implementation of the GMC Micromechanics Model for Multi-Phased Materials With Complex Microstructures

Marek-Jerzy Pindera and Brett A. Bednarcyk
University of Virginia
Charlottesville, Virginia

May 1997

Prepared for
Lewis Research Center
Under Grants NAG3–1377 and NAG3–1319

National Aeronautics and
Space Administration

AN EFFICIENT IMPLEMENTATION OF THE GMC MICROMECHANICS MODEL FOR MULI-PHASED MATERIALS WITH COMPLEX MICROSTRUCTURES

Marek-Jerzy Pindera
Brett A. Bednarcyk

Civil Engineering & Applied Mechanics Department
University of Virginia, Charlottesville, VA 22903

ABSTRACT

An efficient implementation of the generalized method of cells micromechanics model is presented that allows analysis of periodic unidirectional composites characterized by repeating unit cells containing thousands of subcells. The original formulation, given in terms of Hill's strain concentration matrices that relate average subcell strains to the macroscopic strains, is reformulated in terms of the interfacial subcell tractions as the basic unknowns. This is accomplished by expressing the displacement continuity equations in terms of the stresses and then imposing the traction continuity conditions directly. The result is a mixed formulation wherein the unknown interfacial subcell traction components are related to the macroscopic strain components. Because the stress field throughout the repeating unit cell is piece-wise uniform, the imposition of traction continuity conditions directly in the displacement continuity equations, expressed in terms of stresses, substantially reduces the number of unknown subcell traction (and stress) components, and thus the size of the system of equations that must be solved. Further reduction in the size of the system of continuity equations is obtained by separating the normal and shear traction equations in those instances where the individual subcells are, at most, orthotropic. The reformulated version facilitates detailed analysis of the impact of the fiber cross-section geometry and arrangement on the response of multi-phased unidirectional composites with and without evolving damage. Comparison of execution times obtained with the original and reformulated versions of the generalized method of cells demonstrates the new version's efficiency.

INTRODUCTION

The two-dimensional generalized method of cells is a micromechanics model developed by Paley and Aboudi (1992) and Aboudi (1993) for predicting the response of unidirectional metal matrix composites with periodic microstructures. A continuously reinforced composite is modeled as a doubly periodic assemblage of fibers embedded in a matrix phase, Fig. 1. The periodic character of the assemblage allows one to identify a repeating unit cell that is the building block for the entire composite. The properties of this repeating unit cell are thus representative of the properties of the entire assemblage. The repeating unit cell consists of $N_\beta \times N_\gamma$ subcells. Each of these subcells is assumed to be occupied, in general, by a material that exhibits inelastic behavior. The subcell material's inelastic behavior can be modeled by a variety of constitutive theories, including linear viscoelasticity, classical incremental plasticity, or unified viscoplasticity theories. Thus the repeating unit cell consists of $N_\beta \times N_\gamma$ different inelastic materials, i.e., it represents a multi-phased, inelastic composite.

The generalized method of cells allows approximate micromechanical analysis of fairly complicated periodic arrays, including:

- thermomechanical response of multi-phased, metal matrix composites
- modeling of variable fiber shapes
- analysis of different fiber arrays
- modeling of porosities and damage
- modeling of interfacial regions around inclusions, including interfacial degradation

The effective or average stress-strain equations for the composite are constructed through an approximate deformation analysis in each subcell of the repeating unit cell based on a linear representation of the displacement field in terms of local subcell coordinates. Using this approach, the governing field equations within each subcell are satisfied identically in a volumetric sense, while the traction and displacement continuity conditions between adjacent subcells are imposed in an average sense together with an homogenization condition that ensures that the response of a given repeating unit cell is indistinguishable from that of its neighbors. The above analysis establishes the so-called Hill's strain concentration matrix relationships between the average subcell strains and the imposed average or composite strains, that are used in the construction of the composite stress-strain equations (Hill, 1963). The size of the strain concentration matrix is $6N_\beta N_\gamma \times 6N_\beta N_\gamma$ since there are six unknown subcell strains in each of the $N_\beta N_\gamma$ subcells. This matrix must be inverted once if an isothermal mechanical analysis is conducted, and many times if a nonisothermal thermomechanical analysis is conducted with temperature-dependent constitutive properties in the individual subcells. Consequently, this imposes limits on the level of discretization of the repeating unit cell. Practically, the analysis of repeating unit cells larger than 10×10 may become computationally inefficient, particularly if the micromechanical analysis is part of a larger structural analysis.

To enhance the computational efficiency of the generalized method of cells, Orozco (1997) took advantage of the sparse features of the strain concentration matrix in inverting it. The sparse implementation of the generalized method of cells made possible the elastic analysis of periodic fiber arrays characterized by repeating unit cells containing thousands of subcells. Examples were presented for the calculation of the effective properties of unidirectional composites containing up to 100×100 subcells in the repeating unit cell.

Herein, another approach is presented for the efficient implementation of the generalized method of cells. This approach involves reformulating the displacement continuity equations in terms of the interfacial subcell traction components as the basic unknowns in place of the subcell strain components. This reformulation, together with the piece-wise uniform character of the stress field throughout the repeating unit cell and direct imposition of the interfacial traction continuity conditions between the individual subcells, substantially reduces the size of the matrix that must be inverted to express the unknown interfacial subcell tractions (and thus subcell stress components) in terms of the macroscopic strains. This matrix consists of diagonal submatrices and fully-populated off-diagonal submatrices, thereby lending itself to further computational efficiency enhancement through Orozco's sparse implementation approach.

STANDARD FORMULATION OF THE GENERALIZED METHOD OF CELLS

Since the reformulation of the generalized method of cells requires the use of the original equations, we begin by providing a brief outline of the original formulation. We proceed to outline the original micromechanical analysis by first defining the relationships between the average composite and the average subcell stress and strain quantities.

The volume-averaged subcell stress $\bar{\boldsymbol{\sigma}}^{(\beta\gamma)}$ is defined in the usual way,

$$\bar{\boldsymbol{\sigma}}^{(\beta\gamma)} = \frac{1}{V_{\beta\gamma}} \int_{-h_\beta/2}^{+h_\beta/2} \int_{-l_\gamma/2}^{+l_\gamma/2} \boldsymbol{\sigma}^{(\beta\gamma)} d\bar{x}_2^{(\beta)} d\bar{x}_3^{(\gamma)} \tag{1}$$

(where $V_{\beta\gamma} = h_\beta l_\gamma$). Thus the average composite stress $\bar{\boldsymbol{\sigma}}$ is obtained from a weighted sum of the subcell average stresses taken over all the subcells,

$$\bar{\boldsymbol{\sigma}} = \frac{1}{hl} \sum_{\beta=1}^{N_\beta} \sum_{\gamma=1}^{N_\gamma} h_\beta l_\gamma \bar{\boldsymbol{\sigma}}^{(\beta\gamma)} \tag{2}$$

where h and l are the dimensions of the repeating unit cell, Fig. 1. Similarly, the volume-averaged subcell strain $\bar{\boldsymbol{\varepsilon}}^{(\beta\gamma)}$ is given by,

$$\bar{\boldsymbol{\varepsilon}}^{(\beta\gamma)} = \frac{1}{V_{\beta\gamma}} \int_{-h_\beta/2}^{+h_\beta/2} \int_{-l_\gamma/2}^{+l_\gamma/2} \boldsymbol{\varepsilon}^{(\beta\gamma)} d\bar{x}_2^{(\beta)} d\bar{x}_3^{(\gamma)} \tag{3}$$

and the average composite strain $\bar{\boldsymbol{\varepsilon}}$ is obtained from a sweighted sum of the subcell average strains taken over all the subcells,

$$\bar{\boldsymbol{\varepsilon}} = \frac{1}{hl} \sum_{\beta=1}^{N_\beta} \sum_{\gamma=1}^{N_\gamma} h_\beta l_\gamma \bar{\boldsymbol{\varepsilon}}^{(\beta\gamma)} \tag{4}$$

The relationship between average subcell stresses and strains is obtained by volume averaging the constitutive equations used to describe the material behavior in the subcell ($\beta\gamma$),

$$\bar{\boldsymbol{\sigma}}^{(\beta\gamma)} = \boldsymbol{C}^{(\beta\gamma)} \left[\bar{\boldsymbol{\varepsilon}}^{(\beta\gamma)} - \bar{\boldsymbol{\varepsilon}}^{p(\beta\gamma)} - \boldsymbol{\alpha}^{(\beta\gamma)} \Delta T \right] \tag{5}$$

where $\bar{\boldsymbol{\varepsilon}}^{p(\beta\gamma)}$ is the average plastic subcell strain, $\boldsymbol{C}^{(\beta\gamma)}$ is the elastic stiffness matrix, $\boldsymbol{\alpha}^{(\beta\gamma)}$ are the coefficients of thermal expansion, and ΔT is the temperature deviation. The above description of the material behavior is sufficiently general to admit any inelastic constitutive model for the plastic strain $\bar{\boldsymbol{\varepsilon}}^{p(\beta\gamma)}$ in the subcell ($\beta\gamma$). Herein, the classical incremental plasticity theory, reformulated in terms of strains (Mendelson, 1983; Williams and Pindera, 1997) is used to model the inelastic effects.

The effective or average stress-strain equations for the composite are constructed from the definition of the volume-averaged composite stresses, eqn (2), by first expressing the volume-averaged subcell stresses, eqn (1), in terms of the volume-averaged subcell strains using eqn (5). Then, the volume-averaged subcell strains are expressed in terms of the composite strains through the use of Hill's strain concentration matrix relations obtained from the approximate deformation analysis of the individual subcells. This produces the effective stress-strain equations for the composite in the form:

$$\bar{\boldsymbol{\sigma}} = \boldsymbol{C}^* \left(\bar{\boldsymbol{\varepsilon}} - \bar{\boldsymbol{\varepsilon}}^p - \boldsymbol{\alpha}^* \Delta T\right) \tag{6}$$

where $\bar{\boldsymbol{\varepsilon}}^p$ is the average composite plastic strain, $\boldsymbol{C}^*$ is the effective elastic stiffness matrix, and $\boldsymbol{\alpha}^*$ is the effective thermal expansion coefficient vector.

The relationship between the volume-averaged subcell and composite strains, necessary to generate eqn (6), is obtained through an approximate analysis of the deformation fields in each subcell of the repeating unit cell. Towards this end, the displacement field in the individual subcells modeling a continuously reinforced composite is approximated in terms of a linear expansion in the local coordinates $\bar{x}_2^{(\beta)}, \bar{x}_3^{(\gamma)}$ centered at the mid-point of a given subcell,

$$u_i^{(\beta\gamma)} = \omega_i^{(\beta\gamma)} + \bar{x}_2^{(\beta)} \phi_i^{(\beta\gamma)} + \bar{x}_3^{(\gamma)} \psi_i^{(\beta\gamma)} \tag{7}$$

where i = 1, 2, or 3; $\beta = 1, \ldots, N_\beta$; $\gamma = 1, \ldots, N_\gamma$; and $\omega_i^{(\beta\gamma)}$ are the displacement components at the center of each subcell $(\beta\gamma)$, defined at discrete points in the x_2–x_3 plane but treated as continuous functions of the axial coordinate x_1 aligned with the fiber direction. Using the local strain-displacement equations for each subcell, one can easily show that the microvariables $\phi_i^{(\beta\gamma)}$ and $\psi_i^{(\beta\gamma)}$ are related to the subcell strains $\varepsilon_{ij}^{(\beta\gamma)}$. It follows then, that the subcell strains, and therefore stresses, are piece-wise uniform throughout the repeating unit cell. Thus we obtain the following relations between the microvariables $\phi_i^{(\beta\gamma)}$ and $\psi_i^{(\beta\gamma)}$ and the volume-averaged subcell strains $\bar{\varepsilon}_{ij}^{(\beta\gamma)}$,

$$\bar{\varepsilon}_{11}^{(\beta\gamma)} = \frac{\partial \omega_1^{(\beta\gamma)}}{\partial x_1}, \quad \bar{\varepsilon}_{22}^{(\beta\gamma)} = \phi_2^{(\beta\gamma)}, \quad \bar{\varepsilon}_{33}^{(\beta\gamma)} = \psi_3^{(\beta\gamma)} \tag{8a}$$

$$\bar{\varepsilon}_{12}^{(\beta\gamma)} = \frac{1}{2}\left(\phi_1^{(\beta\gamma)} + \frac{\partial \omega_2^{(\beta\gamma)}}{\partial x_1}\right), \quad \bar{\varepsilon}_{13}^{(\beta\gamma)} = \frac{1}{2}\left(\psi_1^{(\beta\gamma)} + \frac{\partial \omega_3^{(\beta\gamma)}}{\partial x_1}\right), \quad \bar{\varepsilon}_{23}^{(\beta\gamma)} = \frac{1}{2}\left(\psi_2^{(\beta\gamma)} + \phi_3^{(\beta\gamma)}\right) \tag{8b}$$

Since the subcell stresses and strains are piece-wise uniform throughout the repeating unit cell, the governing field equations are satisfied identically. The piece-wise uniform character of the stress and strain fields, however, requires that the interfacial traction and displacement continuity between the individual subcells within the repeating unit cell, as well as between the given repeating unit cell and the surrounding cells, be imposed in an average sense. Imposing these displacement continuity conditions and

applying an homogenization condition that ensures that the given cell deforms in an indistinguishable manner from its neighbors, we obtain:

$$\sum_{\beta=1}^{N_\beta} h_\beta \phi_i^{(\beta\gamma)} = h \frac{\partial \omega_i^{(\beta\gamma)}}{\partial x_2} \quad ; \quad \gamma = 1, \ldots, N_\gamma \tag{9a}$$

$$\sum_{\gamma=1}^{N_\gamma} l_\gamma \psi_i^{(\beta\gamma)} = l \frac{\partial \omega_i^{(\beta\gamma)}}{\partial x_3} \quad ; \quad \beta = 1, \ldots, N_\beta \tag{9b}$$

where it can be shown that (Brayshaw, 1994)

$$\frac{\partial \omega_i^{(\beta\gamma)}}{\partial x_j} = \frac{\partial \omega_i}{\partial x_j} \tag{10}$$

for all the subcells. Use of the above relations in the definitions for the average composite strains given in terms of the volume-averaged subcell strains, eqn (4), together with eqns (8) and (9) yields the relations,

$$\bar{\varepsilon}_{ij} = \frac{1}{2}\left(\frac{\partial \omega_i}{\partial x_j} + \frac{\partial \omega_j}{\partial x_i}\right) \tag{11}$$

Thus the uniform axial deformation constraint and the interfacial displacement continuity conditions provide the following relations between the volume-averaged subcell strains and the composite strains,

$$\bar{\varepsilon}_{11}^{(\beta\gamma)} = \bar{\varepsilon}_{11} \, , \quad \beta = 1, \ldots, N_\beta \, ; \quad \gamma = 1, \ldots, N_\gamma \tag{12a}$$

$$\sum_{\beta=1}^{N_\beta} h_\beta \bar{\varepsilon}_{22}^{(\beta\gamma)} = h \bar{\varepsilon}_{22} \, , \quad \gamma = 1, \ldots, N_\gamma \tag{12b}$$

$$\sum_{\beta=1}^{N_\beta} h_\beta \bar{\varepsilon}_{12}^{(\beta\gamma)} = h \bar{\varepsilon}_{12} \, , \quad \gamma = 1, \ldots, N_\gamma \tag{12c}$$

$$\sum_{\gamma=1}^{N_\gamma} l_\gamma \bar{\varepsilon}_{33}^{(\beta\gamma)} = l \bar{\varepsilon}_{33} \, , \quad \beta = 1, \ldots, N_\beta \tag{12d}$$

$$\sum_{\gamma=1}^{N_\gamma} l_\gamma \bar{\varepsilon}_{13}^{(\beta\gamma)} = l \bar{\varepsilon}_{13} \, , \quad \beta = 1, \ldots, N_\beta \tag{12e}$$

$$\sum_{\beta=1}^{N_\beta} \sum_{\gamma=1}^{N_\gamma} h_\beta l_\gamma \bar{\varepsilon}_{23}^{(\beta\gamma)} = h l \bar{\varepsilon}_{23} \tag{12f}$$

This system of equations can be written in the matrix form,

$$\boldsymbol{A}_G \bar{\boldsymbol{\varepsilon}}_s = \boldsymbol{J}\bar{\boldsymbol{\varepsilon}} \tag{13}$$

The matrix $\boldsymbol{A}_G$ contains terms that describe the internal geometry of the repeating unit cell. The vector $\bar{\boldsymbol{\varepsilon}}_s = (\bar{\boldsymbol{\varepsilon}}^{(11)}, ..., \bar{\boldsymbol{\varepsilon}}^{(N_\beta N_\gamma)})$ with dimension $6N_\beta N_\gamma$ contains the six volume-averaged strain components for each of the $N_\beta N_\gamma$ subcells. The matrix $\boldsymbol{J}$ contains the overall cell dimensions.

The displacement continuity conditions, eqns (13), provide $2(N_\beta + N_\gamma) + N_\beta N_\gamma + 1$ equations involving the $6N_\beta N_\gamma$ unknown subcell strains. The imposition of the interfacial traction continuity provides the remaining $5N_\beta N_\gamma - 2(N_\beta + N_\gamma) - 1$ equations for the determination of the unknown subcell strains in terms of the macroscopic strains,

$$\bar{\sigma}_{2i}^{(\beta\gamma)} = \bar{\sigma}_{2i}^{(\hat{\beta}\gamma)} \;:\; \hat{\beta} = \beta + 1 \;\; when \;\; \beta < N_\beta \;\; \text{and} \;\; \hat{\beta} = 1 \;\; when \;\; \beta = N_\beta \,, \;\; \gamma = 1,..., N_\gamma \tag{14a}$$

$$\bar{\sigma}_{3i}^{(\beta\gamma)} = \bar{\sigma}_{3i}^{(\beta\hat{\gamma})} \;:\; \hat{\gamma} = \gamma + 1 \;\; when \;\; \gamma < N_\gamma \;\; \text{and} \;\; \hat{\gamma} = 1 \;\; when \;\; \gamma = N_\gamma \,, \;\; \beta = 1,..., N_\beta \tag{14b}$$

for i=1,2,3. These traction continuity equations can be expressed in matrix form in terms of volume-averaged total, plastic and thermal subcell strains upon use of the volume-averaged subcell constitutive relations, eqn (5),

$$\boldsymbol{A}_M(\bar{\boldsymbol{\varepsilon}}_s - \bar{\boldsymbol{\varepsilon}}_s^p - \bar{\boldsymbol{\varepsilon}}_s^T) = \boldsymbol{0} \tag{15}$$

where $\bar{\boldsymbol{\varepsilon}}_s^p = (\bar{\boldsymbol{\varepsilon}}^{p(11)}, ..., \bar{\boldsymbol{\varepsilon}}^{p(N_\beta N_\gamma)})$, $\bar{\boldsymbol{\varepsilon}}_s^T = (\bar{\boldsymbol{\varepsilon}}^{T(11)}, ..., \bar{\boldsymbol{\varepsilon}}^{T(N_\beta N_\gamma)})$, are the plastic strain and thermal strain vectors, respectively, for all the subcells, $\bar{\boldsymbol{\varepsilon}}^{T(\beta\gamma)} = \boldsymbol{\alpha}^{(\beta\gamma)}\Delta T$, and the matrix $\boldsymbol{A}_M$ contains the elastic constants of the materials in the individual subcells.

Combining eqns (13) and (15), the system of equations relating the subcell strains to the uniformly applied composite strains, obtained from the imposition of the continuity conditions, can be written in compact matrix notation as follows,

$$\tilde{\boldsymbol{A}}\bar{\boldsymbol{\varepsilon}}_s = \tilde{\boldsymbol{K}}\bar{\boldsymbol{\varepsilon}} + \tilde{\boldsymbol{D}}(\bar{\boldsymbol{\varepsilon}}_s^p + \bar{\boldsymbol{\varepsilon}}_s^T) \tag{16}$$

where

$$\tilde{\boldsymbol{A}} = \begin{bmatrix} \boldsymbol{A}_M \\ \boldsymbol{A}_G \end{bmatrix}, \;\; \tilde{\boldsymbol{D}} = \begin{bmatrix} \boldsymbol{A}_M \\ \boldsymbol{0} \end{bmatrix}, \;\; \tilde{\boldsymbol{K}} = \begin{bmatrix} \boldsymbol{0} \\ \boldsymbol{J} \end{bmatrix} \tag{17}$$

The above equations can be solved in order to express the subcell strains in terms of the average strains:

$$\bar{\varepsilon}_s = A\bar{\varepsilon} + D(\bar{\varepsilon}_s^p + \bar{\varepsilon}_s^T) \tag{18}$$

where $A = \tilde{A}^{-1}K$ and $D = \tilde{A}^{-1}\tilde{D}$. The matrix A, in fact, is the resulting Hill's concentration matrix which relates the microstrains to macrostrains. It follows from eqn (18) that the average subcell strains can be expressed in terms of the macroscopic strains and average plastic and thermal subcell strains as follows:

$$\bar{\varepsilon}^{(\beta\gamma)} = A^{(\beta\gamma)}\bar{\varepsilon} + D^{(\beta\gamma)}(\bar{\varepsilon}_s^p + \bar{\varepsilon}_s^T) \tag{19}$$

so that the average subcell stresses become:

$$\bar{\sigma}^{(\beta\gamma)} = C^{(\beta\gamma)}[A^{(\beta\gamma)}\bar{\varepsilon} + D^{(\beta\gamma)}(\bar{\varepsilon}_s^p + \bar{\varepsilon}_s^T) - (\bar{\varepsilon}^{p(\beta\gamma)} + \bar{\varepsilon}^{T(\beta\gamma)})] \tag{20}$$

Using these expressions in the definitions for the macroscopic stresses given in terms of the average subcells stresses, eqn (2), we obtain the following constitutive equation for the composite response,

$$\bar{\sigma} = \frac{1}{hl}\sum_{\beta=1}^{N_\beta}\sum_{\gamma=1}^{N_\gamma} h_\beta l_\gamma C^{(\beta\gamma)}[A^{(\beta\gamma)}\bar{\varepsilon} + D^{(\beta\gamma)}(\bar{\varepsilon}_s^p + \bar{\varepsilon}_s^T) - (\bar{\varepsilon}^{p(\beta\gamma)} + \bar{\varepsilon}^{T(\beta\gamma)})] \tag{21}$$

Comparison of eqns (21) and (6) yields the following expressions for the macroscopic stiffness matrix C^* given in terms of the subcell stiffness matrices $C^{(\beta\gamma)}$ and the subcell strain concentrations matrices $A^{(\beta\gamma)}$,

$$C^* = \frac{1}{hl}\sum_{\beta=1}^{N_\beta}\sum_{\gamma=1}^{N_\gamma} h_\beta l_\gamma C^{(\beta\gamma)}A^{(\beta\gamma)} \tag{22}$$

and for the macroscopic plastic and thermal strains $\bar{\varepsilon}^p$ and $\bar{\varepsilon}^T$ given in terms of the average subcell plastic and thermal strains $\bar{\varepsilon}^{p(\beta\gamma)}$ and $\bar{\varepsilon}^{T(\beta\gamma)}$ and the plastic strain concentration matrices $D^{(\beta\gamma)}$,

$$\bar{\varepsilon}^p = -\frac{1}{hl}(C^*)^{-1}\sum_{\beta=1}^{N_\beta}\sum_{\gamma=1}^{N_\gamma} h_\beta l_\gamma C^{(\beta\gamma)}(D^{(\beta\gamma)}\bar{\varepsilon}_s^p - \bar{\varepsilon}^{p(\beta\gamma)}) \tag{23}$$

$$\bar{\varepsilon}^T = -\frac{1}{hl}(C^*)^{-1}\sum_{\beta=1}^{N_\beta}\sum_{\gamma=1}^{N_\gamma} h_\beta l_\gamma C^{(\beta\gamma)}(D^{(\beta\gamma)}\bar{\varepsilon}_s^T - \bar{\varepsilon}^{T(\beta\gamma)}) \tag{24}$$

Since the evolution of subcell plastic strains depends on the deformation history of the composite, these strains must be determined in an incremental fashion dependent on the particular form of the employed inelastic model for the matrix phase. A detailed presentation of the two-dimensional generalized method of cells analysis can be found in Paley and Aboudi (1992) and Aboudi (1993).

EFFICIENT REFORMULATION OF THE GENERALIZED METHOD OF CELLS

The core of the computational effort in the original formulation of the generalized method of cells lies in evaluating the strain concentration matrices $\boldsymbol{A}$ and $\boldsymbol{D}$ in eqn (18), i.e., solving the $6N_\beta N_\gamma \times 6N_\beta N_\gamma$ system of equations given in eqn (16). The computational effort can be tremendously reduced by expressing the displacement continuity relations, eqns (12b)-(12f), in terms of subcell stresses using the strain-stress equations,

$$\bar{\boldsymbol{\varepsilon}}^{(\beta\gamma)} = \boldsymbol{S}^{(\beta\gamma)}\,\bar{\boldsymbol{\sigma}}^{(\beta\gamma)} + \bar{\boldsymbol{\varepsilon}}^{p(\beta\gamma)} + \boldsymbol{\alpha}^{(\beta\gamma)}\,\Delta T \tag{25}$$

and then imposing the interfacial traction continuity conditions directly in the reformulated interfacial displacement continuity equations. Further reduction can be achieved by separating the relationships between the subcell normal tractions and macroscopic normal strains from the relationships between the subcell shear tractions and macroscopic shear strains. When the subcells are, at most, orthotropic (as is the case here), this separation is possible because of the absence of shear-normal coupling owing to the use of a first order displacement expansion and the imposition of the interfacial continuity conditions in an average sense. The relations between subcell normal tractions and macroscopic normal strains are given first, followed by the corresponding shear relationships.

Relations between subcell normal tractions and macroscopic normal strains

We express eqns (12b) and (12d) in terms of the three subcell normal stresses using eqn (25). The axial normal subcell stress $\bar{\sigma}_{11}^{(\beta\gamma)}$ is then expressed in terms of the common macroscopic strain $\bar{\varepsilon}_{11}$ and the transverse normal subcell stresses $\bar{\sigma}_{22}^{(\beta\gamma)}$ and $\bar{\sigma}_{33}^{(\beta\gamma)}$ using the uniform axial deformation constraint, eqn (12a), and the first of the strain-stress equations (see the Appendix). Defining the common interfacial normal traction $T_{22}^{(\gamma)}$ for a fixed column of subcells $(1\gamma),\ldots,(N_\beta\gamma)$ and $T_{33}^{(\beta)}$ for a fixed row of subcells $(\beta 1),\ldots,(\beta N_\gamma)$ dictated by the interfacial traction continuity conditions,

$$\bar{\sigma}_{22}^{(1\gamma)} = \bar{\sigma}_{22}^{(2\gamma)} = \ldots = \bar{\sigma}_{22}^{(N_\beta\gamma)} = T_{22}^{(\gamma)}\,, \quad \gamma = 1,\ldots, N_\gamma \tag{26}$$

$$\bar{\sigma}_{33}^{(\beta 1)} = \bar{\sigma}_{33}^{(\beta 2)} = \ldots = \bar{\sigma}_{33}^{(\beta N_\gamma)} = T_{33}^{(\beta)}\,, \quad \beta = 1,\ldots, N_\beta \tag{27}$$

the reformulated interfacial displacement continuity conditions become,

$$A_\gamma T_{22}^{(\gamma)} + \sum_{\beta=1}^{N_\beta} h_\beta B_{\beta\gamma} T_{33}^{(\beta)} = h\bar{\varepsilon}_{22} - c_\gamma \bar{\varepsilon}_{11} + d_\gamma \Delta T + p_1^{(\gamma)}\,, \quad \gamma = 1,\ldots, N_\gamma \tag{28}$$

$$\sum_{\gamma=1}^{N_\gamma} l_\gamma B_{\beta\gamma} T_{22}^{(\gamma)} + D_\beta T_{33}^{(\beta)} = l\bar{\varepsilon}_{33} - e_\beta \bar{\varepsilon}_{11} + f_\beta \Delta T + p_2^{(\beta)}\,, \quad \beta = 1,\ldots, N_\beta \tag{29}$$

Equations (28) and (29) can be cast in the matrix form given below,

$$\begin{bmatrix} \boldsymbol{A} & \boldsymbol{B} \\ \boldsymbol{B}' & \boldsymbol{D} \end{bmatrix} \begin{Bmatrix} \boldsymbol{T}_2 \\ \boldsymbol{T}_3 \end{Bmatrix} = \begin{Bmatrix} \boldsymbol{H} \\ \boldsymbol{0} \end{Bmatrix} \bar{\varepsilon}_{22} + \begin{Bmatrix} \boldsymbol{0} \\ \boldsymbol{L} \end{Bmatrix} \bar{\varepsilon}_{33} - \begin{Bmatrix} \boldsymbol{c} \\ \boldsymbol{e} \end{Bmatrix} \bar{\varepsilon}_{11} + \begin{Bmatrix} \boldsymbol{d} \\ \boldsymbol{f} \end{Bmatrix} \Delta T + \begin{Bmatrix} \boldsymbol{P}_1 \\ \boldsymbol{P}_2 \end{Bmatrix} \tag{30}$$

where $\boldsymbol{A}$, $\boldsymbol{B}$, $\boldsymbol{B}'$ and $\boldsymbol{D}$ are $N_\gamma \times N_\gamma$, $N_\gamma \times N_\beta$, $N_\beta \times N_\gamma$, and $N_\beta \times N_\beta$ matrices, respectively, whose structure and elements are given below; $\boldsymbol{T}_2 = [T_{22}^{(1)}, \ldots, T_{22}^{(N_\gamma)}]$ and $\boldsymbol{T}_3 = [T_{33}^{(1)}, \ldots, T_{33}^{(N_\beta)}]$ contain the N_γ and N_β unknown normal tractions in the individual columns and rows of the unit cell, respectively; $\boldsymbol{H}$ and $\boldsymbol{L}$ are $N_\gamma \times 1$ and $N_\beta \times 1$ vectors whose elements are the cell dimensions h and l, respectively; and the vectors $\boldsymbol{c} = [c_1, \ldots, c_{N_\gamma}]$, $\boldsymbol{d} = [d_1, \ldots, d_{N_\gamma}]$, $\boldsymbol{e} = [e_1, \ldots, e_{N_\beta}]$, $\boldsymbol{f} = [f_1, \ldots, f_{N_\beta}]$, $\boldsymbol{P}_1 = [p_1^{(1)}, \ldots, p_1^{(N_\gamma)}]$, $\boldsymbol{P}_2 = [p_2^{(1)}, \ldots, p_2^{(N_\beta)}]$ contain elements also provided below.

$$\boldsymbol{A} = \begin{bmatrix} A_1 & 0 & \cdot & \cdot & 0 \\ 0 & A_2 & \cdot & \cdot & 0 \\ \cdot & \cdot & \cdot & \cdot & \cdot \\ \cdot & \cdot & \cdot & \cdot & \cdot \\ 0 & 0 & \cdot & \cdot & A_{N_\gamma} \end{bmatrix} \qquad \boldsymbol{B} = \begin{bmatrix} h_1 B_{11} & h_2 B_{21} & \cdot & \cdot & h_{N_\beta} B_{N_\beta 1} \\ h_1 B_{12} & h_2 B_{22} & \cdot & \cdot & h_{N_\beta} B_{N_\beta 2} \\ \cdot & \cdot & \cdot & \cdot & \cdot \\ \cdot & \cdot & \cdot & \cdot & \cdot \\ h_1 B_{1N_\gamma} & h_2 B_{2N_\gamma} & \cdot & \cdot & h_{N_\beta} B_{N_\beta N_\gamma} \end{bmatrix}$$

$$\boldsymbol{B}' = \begin{bmatrix} l_1 B_{11} & l_2 B_{12} & \cdot & \cdot & l_{N_\gamma} B_{1N_\gamma} \\ l_1 B_{21} & l_2 B_{22} & \cdot & \cdot & l_{N_\gamma} B_{2N_\gamma} \\ \cdot & \cdot & \cdot & \cdot & \cdot \\ \cdot & \cdot & \cdot & \cdot & \cdot \\ l_1 B_{N_\beta 1} & l_2 B_{N_\beta 2} & \cdot & \cdot & l_{N_\gamma} B_{N_\beta N_\gamma} \end{bmatrix} \qquad \boldsymbol{D} = \begin{bmatrix} D_1 & 0 & \cdot & \cdot & 0 \\ 0 & D_2 & \cdot & \cdot & 0 \\ \cdot & \cdot & \cdot & \cdot & \cdot \\ \cdot & \cdot & \cdot & \cdot & \cdot \\ 0 & 0 & \cdot & \cdot & D_{N_\beta} \end{bmatrix}$$

$$A_\gamma = \sum_{\beta=1}^{N_\beta} h_\beta \left(S_{22}^{(\beta\gamma)} - \frac{S_{12}^{(\beta\gamma)^2}}{S_{11}^{(\beta\gamma)}} \right), \quad B_{\beta\gamma} = S_{23}^{(\beta\gamma)} - \frac{S_{12}^{(\beta\gamma)} S_{13}^{(\beta\gamma)}}{S_{11}^{(\beta\gamma)}}, \quad D_\beta = \sum_{\gamma=1}^{N_\gamma} l_\gamma \left(S_{33}^{(\beta\gamma)} - \frac{S_{13}^{(\beta\gamma)^2}}{S_{11}^{(\beta\gamma)}} \right) \tag{31a}$$

$$c_\gamma = \sum_{\beta=1}^{N_\beta} h_\beta \frac{S_{12}^{(\beta\gamma)}}{S_{11}^{(\beta\gamma)}}, \quad d_\gamma = \sum_{\beta=1}^{N_\beta} h_\beta \left(\frac{S_{12}^{(\beta\gamma)}}{S_{11}^{(\beta\gamma)}} \alpha_{11}^{(\beta\gamma)} - \alpha_{22}^{(\beta\gamma)} \right), \quad p_1^{(\gamma)} = \sum_{\beta=1}^{N_\beta} h_\beta \left(\frac{S_{12}^{(\beta\gamma)}}{S_{11}^{(\beta\gamma)}} \bar{\varepsilon}_{11}^{p(\beta\gamma)} - \bar{\varepsilon}_{22}^{p(\beta\gamma)} \right) \tag{31b}$$

$$e_\beta = \sum_{\gamma=1}^{N_\gamma} l_\gamma \frac{S_{13}^{(\beta\gamma)}}{S_{11}^{(\beta\gamma)}}, \quad f_\beta = \sum_{\gamma=1}^{N_\gamma} l_\gamma \left(\frac{S_{13}^{(\beta\gamma)}}{S_{11}^{(\beta\gamma)}} \alpha_{11}^{(\beta\gamma)} - \alpha_{33}^{(\beta\gamma)} \right), \quad p_2^{(\beta)} = \sum_{\gamma=1}^{N_\gamma} l_\gamma \left(\frac{S_{13}^{(\beta\gamma)}}{S_{11}^{(\beta\gamma)}} \bar{\varepsilon}_{11}^{p(\beta\gamma)} - \bar{\varepsilon}_{33}^{p(\beta\gamma)} \right) \tag{31c}$$

Equation (30) forms the core of the computational effort in the reformulated generalized method of cells. The system of equations to be solved contains $N_\beta + N_\gamma$ unknowns in place of the $6N_\beta N_\gamma$ unknowns

in the original version. Additional relations between subcell shear tractions and macroscopic shear strains do remain to be established to complete the reformulation. However, the computational effort involved in calculating the subcell shear tractions in terms of the macroscopic shear strains is minimal due to the absence of shear-normal and shear-shear coupling as illustrated next. Furthermore, we note that eqn (30) can be further reduced by expressing it either in terms of $\boldsymbol{T}_2$ or $\boldsymbol{T}_3$. However, as will be illustrated in the next section, this reduction is offset by a greater number of matrix operations necessary to calculate the effective composite response, thus leading to increased efficiency only in certain circumstances.

Relations between subcell shear tractions and macroscopic shear strains

To obtain the axial shear relations, we express eqns (12c) and (12e) in terms of the subcell axial shear stresses using eqn (25). Owing to the absence of normal-shear and shear-shear coupling in orthotropic materials, these relations involve only the subcell shear stress and macroscopic shear strain quantities in the respective planes (see the Appendix). Defining the common interfacial shear traction $T_{21}^{(\gamma)}$ for a fixed column of subcells $(1\gamma),\ldots,(N_\beta\gamma)$ and $T_{31}^{(\beta)}$ for a fixed row of subcells $(\beta 1),\ldots,(\beta N_\gamma)$ dictated by the interfacial traction continuity conditions, and utilizing the symmetry of the stress tensor,

$$\bar{\sigma}_{21}^{(1\gamma)} = \bar{\sigma}_{21}^{(2\gamma)} = \ldots = \bar{\sigma}_{21}^{(N_\beta\gamma)} = T_{21}^{(\gamma)} = T_{12}^{(\gamma)}\ , \quad \gamma = 1,\ldots, N_\gamma \tag{32}$$

$$\bar{\sigma}_{31}^{(\beta 1)} = \bar{\sigma}_{31}^{(\beta 2)} = \ldots = \bar{\sigma}_{31}^{(\beta N_\gamma)} = T_{31}^{(\beta)} = T_{13}^{(\beta)}\ , \quad \beta = 1,\ldots, N_\beta \tag{33}$$

the reformulated interfacial displacement continuity conditions become,

$$\frac{1}{2}\Big(\sum_{\beta=1}^{N_\beta} h_\beta S_{66}^{(\beta\gamma)}\Big) T_{12}^{(\gamma)} = h\bar{\varepsilon}_{12} - \sum_{\beta=1}^{N_\beta} h_\beta \bar{\varepsilon}_{12}^{p(\beta\gamma)}\ , \quad \gamma = 1,\ldots, N_\gamma \tag{34}$$

$$\frac{1}{2}\Big(\sum_{\gamma=1}^{N_\gamma} l_\gamma S_{55}^{(\beta\gamma)}\Big) T_{13}^{(\beta)} = l\bar{\varepsilon}_{13} - \sum_{\gamma=1}^{N_\gamma} l_\gamma \bar{\varepsilon}_{13}^{p(\beta\gamma)}\ , \quad \beta = 1,\ldots, N_\beta \tag{35}$$

Thus the solution for the subcell interfacial shear tractions $T_{12}^{(\gamma)}$ and $T_{13}^{(\beta)}$ is readily obtained in terms of the respective macroscopic shear strains and subcell plastic shear strains with minimum computational effort.

To obtain the remaining transverse shear relation, we express eqn (12f) in terms of the subcell transverse shear stresses using eqn (25). Owing to the absence of normal-shear and shear-shear coupling in orthotropic materials, this relation involves only the subcell shear stress and macroscopic shear strain quantities in the transverse plane (see the Appendix). Defining the common interfacial shear traction $T_{23}^{(\gamma)}$ for a fixed column of subcells $(1\gamma),\ldots,(N_\beta\gamma)$ and $T_{32}^{(\beta)}$ for a fixed row of subcells $(\beta 1),\ldots,(\beta N_\gamma)$ dictated by the interfacial traction continuity conditions,

$$\bar{\sigma}_{23}^{(1\gamma)} = \bar{\sigma}_{23}^{(2\gamma)} = \ldots = \bar{\sigma}_{23}^{(N_\beta\gamma)} = T_{23}^{(\gamma)}\ , \quad \gamma = 1,\ldots, N_\gamma \tag{36}$$

$$\bar{\sigma}_{32}^{(\beta 1)} = \bar{\sigma}_{32}^{(\beta 2)} = \ldots = \bar{\sigma}_{32}^{(\beta N_\gamma)} = T_{32}^{(\beta)}\ , \quad \beta = 1,\ldots, N_\beta \tag{37}$$

and utilizing the stress tensor's symmetry, i.e., $\bar{\sigma}_{23}^{(\beta\gamma)} = \bar{\sigma}_{32}^{(\beta\gamma)}$, so that $T_{23}^{(\gamma)} = T_{32}^{(\beta)} = T_{23}$ for all combinations of $\beta = 1,\ldots,N_\beta$ and $\gamma = 1,\ldots,N_\gamma$, the reformulated interfacial displacement continuity condition becomes,

$$\frac{1}{2}\Big(\sum_{\beta=1}^{N_\beta}\sum_{\gamma=1}^{N_\gamma} h_\beta l_\gamma S_{44}^{(\beta\gamma)}\Big) T_{23} = h\bar{l}\bar{\varepsilon}_{23} - \sum_{\beta=1}^{N_\beta}\sum_{\gamma=1}^{N_\gamma} h_\beta l_\gamma \bar{\varepsilon}_{23}^{p(\beta\gamma)} \tag{38}$$

Macroscopic constitutive equations

The macroscopic constitutive equations for the composite are readily determined in the form of eqn (6) by first solving eqns (30), (34), (35), and (38) for the unknown interfacial subcell tractions (and thus subcell stresses), and then using the resulting expressions for the subcell stresses given in terms of the macroscopic strains and subcell plastic strains in the definitions for the macroscopic stresses, eqn (2). To determine the explicit expressions for the effective stiffness moduli, plastic and thermal strains in terms of the individual subcell moduli, plastic strains, thermal expansion coefficients and geometry based on the reformulated approach, we start with the solution of eqn (30). The solutions for $T_{22}^{(\gamma)}$ and $T_{33}^{(\beta)}$, and thus $\bar{\sigma}_{22}^{(\beta\gamma)}$ and $\bar{\sigma}_{33}^{(\beta\gamma)}$ (see interfacial traction continuity equations (26) and (27)), are obtained in terms of the inverse of the ***ABB'D*** matrix elements appearing on the left hand side of eqn (30), denoted by $\boldsymbol{m}$, and elements of the vectors on the right hand side of eqn (30). The knowledge of these average subcell stresses provides the solution for $\bar{\sigma}_{11}^{(\beta\gamma)}$ as well. The resulting relations between the average subcell normal stresses, the macroscopic strains and plastic and thermal subcell strains are,

$$\bar{\sigma}_{11}^{(\beta\gamma)} = a_1^{(\beta\gamma)}\bar{\varepsilon}_{11} + b_1^{(\beta\gamma)}\bar{\varepsilon}_{22} + c_1^{(\beta\gamma)}\bar{\varepsilon}_{33} + \Gamma_1^{(\beta\gamma)}\Delta T + \Phi_1^{(\beta\gamma)} \tag{39}$$

$$\bar{\sigma}_{22}^{(\beta\gamma)} = a_2^{(\gamma)}\bar{\varepsilon}_{11} + b_2^{(\gamma)}\bar{\varepsilon}_{22} + c_2^{(\gamma)}\bar{\varepsilon}_{33} + \Gamma_2^{(\gamma)}\Delta T + \Phi_2^{(\gamma)} \tag{40}$$

$$\bar{\sigma}_{33}^{(\beta\gamma)} = a_3^{(\beta)}\bar{\varepsilon}_{11} + b_3^{(\beta)}\bar{\varepsilon}_{22} + c_3^{(\beta)}\bar{\varepsilon}_{33} + \Gamma_3^{(\beta)}\Delta T + \Phi_3^{(\beta)} \tag{41}$$

where

$$a_1^{(\beta\gamma)} = \frac{1}{S_{11}^{(\beta\gamma)}}[1 - S_{12}^{(\beta\gamma)}a_2^{(\gamma)} - S_{13}^{(\beta\gamma)}a_3^{(\beta)}]\ , \quad b_1^{(\beta\gamma)} = -\frac{1}{S_{11}^{(\beta\gamma)}}[S_{12}^{(\beta\gamma)}b_2^{(\gamma)} + S_{13}^{(\beta\gamma)}b_3^{(\beta)}]$$

$$c_1^{(\beta\gamma)} = -\frac{1}{S_{11}^{(\beta\gamma)}}[S_{12}^{(\beta\gamma)}c_2^{(\gamma)} + S_{13}^{(\beta\gamma)}c_3^{(\beta)}] \tag{42a}$$

$$\Gamma_1^{(\beta\gamma)} = -\frac{1}{S_{11}^{(\beta\gamma)}}[\alpha_{11}^{(\beta\gamma)} + S_{12}^{(\beta\gamma)}\Gamma_2^{(\gamma)} + S_{13}^{(\beta\gamma)}\Gamma_3^{(\beta)}]\ , \quad \Phi_1^{(\beta\gamma)} = -\frac{1}{S_{11}^{(\beta\gamma)}}[\bar{\varepsilon}_{11}^{p(\beta\gamma)} + S_{12}^{(\beta\gamma)}\Phi_2^{(\gamma)} + S_{13}^{(\beta\gamma)}\Phi_3^{(\beta)}] \tag{42b}$$

$$a_2^{(\gamma)} = -\sum_{\alpha=1}^{N_\gamma} m_{(\gamma,\alpha)} c_\alpha - \sum_{\alpha=1}^{N_\beta} m_{(\gamma,N_\gamma+\alpha)} e_\alpha\,, \quad b_2^{(\gamma)} = h\sum_{\alpha=1}^{N_\gamma} m_{(\gamma,\alpha)}\,, \quad c_2^{(\gamma)} = l\sum_{\alpha=1}^{N_\beta} m_{(\gamma,N_\gamma+\alpha)} \tag{43a}$$

$$\Gamma_2^{(\gamma)} = \sum_{\alpha=1}^{N_\gamma} m_{(\gamma,\alpha)} d_\alpha + \sum_{\alpha=1}^{N_\beta} m_{(\gamma,N_\gamma+\alpha)} f_\alpha\,, \quad \Phi_2^{(\gamma)} = \sum_{\alpha=1}^{N_\gamma} m_{(\gamma,\alpha)} p_1^{(\alpha)} + \sum_{\alpha=1}^{N_\beta} m_{(\gamma,N_\gamma+\alpha)} p_2^{(\alpha)} \tag{43b}$$

$$a_3^{(\beta)} = -\sum_{\alpha=1}^{N_\gamma} m_{(N_\gamma+\beta,\alpha)} c_\alpha - \sum_{\alpha=1}^{N_\beta} m_{(N_\gamma+\beta,N_\gamma+\alpha)} e_\alpha\,, \quad b_3^{(\beta)} = h\sum_{\alpha=1}^{N_\gamma} m_{(N_\gamma+\beta,\alpha)}\,, \quad c_3^{(\beta)} = l\sum_{\alpha=1}^{N_\beta} m_{(N_\gamma+\beta,N_\gamma+\alpha)} \tag{44a}$$

$$\Gamma_3^{(\beta)} = \sum_{\alpha=1}^{N_\gamma} m_{(N_\gamma+\beta,\alpha)} d_\alpha + \sum_{\alpha=1}^{N_\beta} m_{(N_\gamma+\beta,N_\gamma+\alpha)} f_\alpha\,, \quad \Phi_3^{(\beta)} = \sum_{\alpha=1}^{N_\gamma} m_{(N_\gamma+\beta,\alpha)} p_1^{(\alpha)} + \sum_{\alpha=1}^{N_\beta} m_{(N_\gamma+\beta,N_\gamma+\alpha)} p_2^{(\alpha)} \tag{44b}$$

Substituting eqns (39)-(41) in the definitions for the average subcell normal stresses given by the first three of eqns (2), we obtain the macroscopic normal constitutive equations of the form given by eqn (6). The elements of the macroscopic elastic stiffness matrix $\boldsymbol{C}^*$, the macroscopic thermal expansion coefficient vector $\boldsymbol{\alpha}^*$ and the macroscopic plastic strain $\bar{\boldsymbol{\varepsilon}}^p$, are explicitly given below in terms of the subcell material and geometric parameters and subcell plastic strains. It is easily verified through numerical experiments that, despite appearance to the contrary, the stiffness matrix $\boldsymbol{C}^*$ is symmetric.

$$\begin{bmatrix} C_{11}^* & C_{12}^* & C_{13}^* \\ C_{21}^* & C_{22}^* & C_{23}^* \\ C_{31}^* & C_{32}^* & C_{33}^* \end{bmatrix} = \begin{bmatrix} \frac{1}{hl}\sum_{\gamma=1}^{N_\gamma}\sum_{\beta=1}^{N_\beta} h_\beta l_\gamma a_1^{(\beta\gamma)} & \frac{1}{hl}\sum_{\gamma=1}^{N_\gamma}\sum_{\beta=1}^{N_\beta} h_\beta l_\gamma b_1^{(\beta\gamma)} & \frac{1}{hl}\sum_{\gamma=1}^{N_\gamma}\sum_{\beta=1}^{N_\beta} h_\beta l_\gamma c_1^{(\beta\gamma)} \\ \frac{1}{l}\sum_{\gamma=1}^{N_\gamma} l_\gamma a_2^{(\gamma)} & \frac{1}{l}\sum_{\gamma=1}^{N_\gamma} l_\gamma b_2^{(\gamma)} & \frac{1}{l}\sum_{\gamma=1}^{N_\gamma} l_\gamma c_2^{(\gamma)} \\ \frac{1}{h}\sum_{\beta=1}^{N_\beta} h_\beta a_3^{(\beta)} & \frac{1}{h}\sum_{\beta=1}^{N_\beta} h_\beta b_3^{(\beta)} & \frac{1}{h}\sum_{\beta=1}^{N_\beta} h_\beta c_3^{(\beta)} \end{bmatrix} \tag{45}$$

$$\begin{Bmatrix} \alpha_{11}^* \\ \alpha_{22}^* \\ \alpha_{33}^* \end{Bmatrix} = -\begin{bmatrix} C_{11}^* & C_{12}^* & C_{13}^* \\ C_{21}^* & C_{22}^* & C_{23}^* \\ C_{31}^* & C_{32}^* & C_{33}^* \end{bmatrix}^{-1} \begin{Bmatrix} \frac{1}{hl}\sum_{\gamma=1}^{N_\gamma}\sum_{\beta=1}^{N_\beta} h_\beta l_\gamma \Gamma_1^{(\beta\gamma)} \\ \frac{1}{l}\sum_{\gamma=1}^{N_\gamma} l_\gamma \Gamma_2^{(\gamma)} \\ \frac{1}{h}\sum_{\beta=1}^{N_\beta} h_\beta \Gamma_3^{(\beta)} \end{Bmatrix}, \quad \begin{Bmatrix} \bar{\varepsilon}_{11}^p \\ \bar{\varepsilon}_{22}^p \\ \bar{\varepsilon}_{33}^p \end{Bmatrix} = -\begin{bmatrix} C_{11}^* & C_{12}^* & C_{13}^* \\ C_{21}^* & C_{22}^* & C_{23}^* \\ C_{31}^* & C_{32}^* & C_{33}^* \end{bmatrix}^{-1} \begin{Bmatrix} \frac{1}{hl}\sum_{\gamma=1}^{N_\gamma}\sum_{\beta=1}^{N_\beta} h_\beta l_\gamma \Phi_1^{(\beta\gamma)} \\ \frac{1}{l}\sum_{\gamma=1}^{N_\gamma} l_\gamma \Phi_2^{(\gamma)} \\ \frac{1}{h}\sum_{\beta=1}^{N_\beta} h_\beta \Phi_3^{(\beta)} \end{Bmatrix} \tag{46}$$

Similarly, the relations between the average subcell shear stresses, plastic strains and macroscopic strains are obtained from eqns (34), (35) and (38) in a straightforward fashion in the form (taking into account the interfacial traction continuity conditions (32), (33) and (36), (37)),

$$\bar{\sigma}_{12}^{(\beta\gamma)} = \frac{1}{E_\gamma}[h\bar{\varepsilon}_{12} - p_{12}^{(\gamma)}] \tag{47}$$

$$\bar{\sigma}_{13}^{(\beta\gamma)} = \frac{1}{F_\beta}[l\bar{\varepsilon}_{13} - p_{13}^{(\beta)}] \tag{48}$$

$$\bar{\sigma}_{23}^{(\beta\gamma)} = \frac{1}{G}[hl\bar{\varepsilon}_{23} - p_{23}] \tag{49}$$

where

$$E_\gamma = \frac{1}{2}\sum_{\beta=1}^{N_\beta} h_\beta S_{66}^{(\beta\gamma)} \ , \quad p_{12}^{(\gamma)} = \sum_{\beta=1}^{N_\beta} h_\beta \bar{\varepsilon}_{12}^{p(\beta\gamma)} \tag{50}$$

$$F_\beta = \frac{1}{2}\sum_{\gamma=1}^{N_\gamma} l_\gamma S_{55}^{(\beta\gamma)} \ , \quad p_{13}^{(\beta)} = \sum_{\gamma=1}^{N_\gamma} l_\gamma \bar{\varepsilon}_{13}^{p(\beta\gamma)} \tag{51}$$

$$G = \frac{1}{2}\sum_{\gamma=1}^{N_\gamma}\sum_{\beta=1}^{N_\beta} h_\beta l_\gamma S_{44}^{(\beta\gamma)} \ , \quad p_{23} = \sum_{\gamma=1}^{N_\gamma}\sum_{\beta=1}^{N_\beta} h_\beta l_\gamma \bar{\varepsilon}_{23}^{p(\beta\gamma)} \tag{52}$$

Substituting eqns (47)-(49) in the definitions for the average subcell shear stresses given by the last three of eqns (2), we obtain the macroscopic shear constitutive equations of the form given by eqn (6). The elements of the macroscopic elastic stiffness matrix $\boldsymbol{C}^*$ and the macroscopic plastic strain $\bar{\boldsymbol{\varepsilon}}^p$ are explicitly given in terms of the subcell material and geometric parameters, and plastic strains as follows,

$$\begin{bmatrix} C_{44}^* & 0 & 0 \\ 0 & C_{55}^* & 0 \\ 0 & 0 & C_{66}^* \end{bmatrix} = \begin{bmatrix} \frac{1}{2}\frac{hl}{G} & 0 & 0 \\ 0 & \frac{1}{2}\frac{l}{h}\sum_{\beta=1}^{N_\beta}\frac{h_\beta}{F_\beta} & 0 \\ 0 & 0 & \frac{1}{2}\frac{h}{l}\sum_{\gamma=1}^{N_\gamma}\frac{l_\gamma}{E_\gamma} \end{bmatrix} \tag{53}$$

$$\begin{Bmatrix} \bar{\varepsilon}_{23}^p \\ \bar{\varepsilon}_{13}^p \\ \bar{\varepsilon}_{12}^p \end{Bmatrix} = \begin{Bmatrix} \frac{1}{2C_{44}^*}\frac{p_{23}}{G} \\ \frac{1}{2C_{55}^* h}\sum_{\beta=1}^{N_\beta}\frac{h_\beta}{F_\beta}p_{13}^{(\beta)} \\ \frac{1}{2C_{66}^* l}\sum_{\gamma=1}^{N_\gamma}\frac{l_\gamma}{E_\gamma}p_{12}^{(\gamma)} \end{Bmatrix} \tag{54}$$

NUMERICAL RESULTS

We begin this section by comparing the times required by the original and reformulated versions of the generalized method of cells to generate the thermal heat-up response of a unidirectional silicon carbide/titanium aluminide (SiC/TiAl) composite. In the presence of temperature-dependent thermoelastic properties of the individual constituents, as is the case here, this is the most computationally demanding case since the solutions to the continuity equations in the original and reformulated versions, eqns (16) and (30) respectively, have to be generated at each thermal load increment. The temperature-dependent material parameters of the constituents are given in Table 1. The SiC fiber is treated as elastic while the titanium aluminide matrix is treated as elastic-plastic with bilinear hardening. The fiber volume fraction of 0.25 was employed in the calculations and the unit cell was composed of a square fiber embedded in a square array. The thermal heat-up response was generated for several unit cells with a progressively greater number of subcells without changing the actual cell geometry. This was accomplished by subdividing each of the four subcells in the original repeating unit cell into increasingly greater numbers of subcells. Therefore, the thermal heat-up response obtained from repeating unit cells with different subcell discretization levels was expected to remain the same for both versions of the generalized method of cells, which provided a check on the generated results. This is illustrated in Fig. 2.

The comparison of the CPU times required by the two versions of the generalized method of cells to simulate the thermal heat up of the SiC/TiAl composite from 24°C to 815°C is provided in Table 2. These results were generated on an IBM RISC System/6000, Machine Type 7012 (Model 39H). The CPU times obtained using the original version of the generalized method of cells are given for unit cells containing up to 12×12 subcells. The CPU times for unit cells containing more than this number of subcells were not generated due to excessively long execution times required for their analysis. Alternatively, CPU times obtained using the reformulated generalized method of cells were easily determined for unit cells with as many as 100×100 subcells. In addition to the dramatic reduction in the computational time evident in the results generated by the reformulated version, it must be pointed out that the size of the unit cell that can be analyzed using the original version is limited by the storage capacity of the employed machine. Thus while unit cells consisting of 100×100 subcells can readily be analyzed using the reformulated version, the maximum number of subcells employed in the original version is not nearly as large. This can be easily understood by recalling that while the size of the matrix that must be inverted in the original version is $6N_\beta N_\gamma \times 6N_\beta N_\gamma$, the size of the corresponding matrix in the reformulated version is only $(N_\beta + N_\gamma) \times (N_\beta + N_\gamma)$. Thus the difference in the size of the matrices that must be inverted in the two versions increases rapidly with increasing number of subcells. It must be mentioned that further reduction in the size of the strain concentration matrix in the original version could be attained by explicitly taking into account the commonality of the axial strain in all the subcells, and by separating the normal and shear contributions. However, this would not change the $N_\beta N_\gamma \times N_\beta N_\gamma$ order of magnitude of the size of the strain concentration matrix in the original version.

We note that under certain circumstances, a further improvement in computational efficiency can be attained by expressing the system of equations (30) either in terms of $\boldsymbol{T}_2$ or $\boldsymbol{T}_3$. In this case, the

calculation of the effective properties and thermal and plastic strains must be reformulated (the details of which are not included here). However, as mentioned previously, the reduction in the size of eqn (30) offered by this is offset by an increased number of matrix operations. For instance, for the thermal heat-up problem considered above, the execution times obtained using the system of equations (30) and its reduced counterpart are approximately the same for unit cells with up to 100×100 subcells. Increasing the number of subcells to 300×300 does result in an increased efficiency of the reduced system of equations by over a factor of two (55,556 vs. 22,229 CPU seconds for the unreduced and reduced system of equations (30), respectively). However, this increase is obtained only for unit cells containing a sufficiently large number of subcells when the system of equations (30) is solved at every load increment, as in the case of temperature-dependent elastic properties of the constituent phases. When the coefficients appearing on the left side of eqn (30) remain constant during the loading history, as in the case of isothermal mechanical loading, reducing the system of equations (30) further offers no advantage. In fact, for the boron/aluminum composite considered next, transverse loading of a unit cell with a square fiber containing 300×300 subcells required 6,521 and 31,306 CPU seconds using the unreduced and reduced system of equations, respectively, almost a five-fold deterioration in the computations efficiency.

Next, we present numerical examples that illustrate the capability of the reformulated generalized method of cells to efficiently model the response of unidirectional metal matrix composites with detailed fiber geometries. In particular, we consider circular, elliptical (with an aspect ratio of 2.5), hexagonal, diamond and square fibers embedded in square arrays (i.e., square repeating unit cells). To obtain true cross-sectional shapes of these fibers, unit cells containing 120×120, 68×68, 102×102, 102×102, and 4×4 subcells were constructed for the circular, elliptical, hexagonal, diamond, and square fibers, respectively, Fig. 3. The properties of the fiber and matrix phases were those of an elastic boron fiber and an elastic-plastic aluminum matrix with bilinear hardening given in Table 3. Two hardening slopes for the aluminum matrix were employed in the calculations, whose magnitudes were 1/10,000 and 1/5 of the elastic Young's modulus. The smaller hardening slope produces a response which is nearly elastic-perfectly plastic, with practically no apparent strain hardening. Figure 4 presents the stress-strain curves of the constituent phases employed in the calculations to generate the composite stress-strain response of the different repeating unit cells under transverse normal loading. Transverse normal loading was chosen because previous investigations have revealed that differences in the response of composites with different fiber shapes are most dramatic under this manner of loading (Arnold, et al., 1996).

Figure 5 presents the transverse response of unit cells containing 0.25 volume fraction of the five differently-shaped fibers embedded in the aluminum matrix with the low and the high rates of strain hardening. In the case of the hexagonal and elliptical fibers, the transverse loading was applied in both of the principal material directions x_2 and x_3 due to the cross-sectional differences along these directions. When the aluminum matrix exhibits no hardening, Fig. 5a, the effect of the fiber cross-section shape on the transverse response is only evident, and to a very limited extent, in the elastic and the initial yielding regions, with virtually no differences observed when the matrix is fully yielded. In the elastic region, the transverse response of the unit cell with the elliptical fiber is somewhat stiffer in the x_3 direction than the

response of the remaining unit cells, however once yielding initiates this difference vanishes. The stiffer response is expected since the major axis of the elliptical fiber lies along the x_3 direction. Alternatively, when the aluminum matrix strain hardens, Fig. 5b, the fiber shape has a more pronounced effect on the transverse response in the plastic region. Substantial differences are now observed in the x_2 and x_3 direction responses of the unit cell with the elliptical fiber. The response of this unit cell in both directions is stiffer than the responses of the remaining unit cells. Among the remaining unit cells, the one with the square fiber exhibits the stiffest response which is slightly higher than the rest. No discernible differences are observed among the responses of the unit cells with diamond, hexagonal and circular fibers.

Increasing the fiber volume fraction further accentuates the differences in the composite's transverse response due to the fiber's cross-sectional shape. Figure 6 shows the results corresponding to those provided in Fig. 5 when the fiber volume fraction is increased to 0.30. This fiber volume fraction is close to the maximum allowable for the unit cell with the elliptical fiber, which is limited by the contact of fibers along the major axis in two adjacent cells. This contact occurs when the fiber volume fraction is 0.31 in the case of fibers with an aspect ratio of 2.5, which is the present situation. When the aluminum matrix exhibits no hardening, Fig. 6a, the effect of the fiber cross-sectional shape on the transverse response in the plastic region becomes discernible, with the square and elliptical fibers being the most effective in increasing the flow stress of the composite, and the diamond, hexagonal and circular fibers the least effective. When the aluminum matrix strain hardens, Fig. 6b, the nearly touching elliptical fibers produce the stiffest overall transverse response, with a substantially greater difference in the x_2 and x_3 directions than that observed at the lower fiber volume fraction, Fig. 5b. The responses of the unit cells with the remaining fibers are substantially lower, and the differences due to the fiber cross-sectional shape somewhat more pronounced than in the 0.25 fiber volume fraction cases. Among these responses, the stiffest response is observed for the unit cell with the square fiber and the most compliant response for the unit cell with the circular fiber.

Figure 7 presents the results that correspond to those shown in the preceding two figures when the fiber volume fraction is further increased to 0.40. This fiber volume fraction exceeds the maximum allowable volume fraction for the employed elliptical fibers, and thus the results are limited to unit cells with square, diamond, hexagonal and circular fibers. In the case of the aluminum matrix with no hardening, Fig. 7a, a substantial difference between the unit cell with the square fiber and the remaining unit cells is now apparent in the plastic region. The square fiber provides a 50% increase in the transverse flow stress of the composite relative to that of the diamond and circular fibers. The transverse response of the unit cell with the hexagonal fiber is essentially the same for both directions of loading and lies above the response of the unit cells with the diamond and circular fibers. It is characterized by slight strain hardening which produces a transverse stress at the strain of 1% that is approximately 18% higher than the flow stress of the unit cells with the diamond and circular fibers. When the aluminum matrix strain hardens, Fig. 7b, increasing the fiber volume fraction from 0.30 to 0.40 also increases the differences in the plastic regime due to the fiber cross-sectional shape. As in the preceding cases, the square fiber produces the stiffest response, while the circular fiber the most compliant. The response of the unit cell with the diamond

fiber falls below that of the unit cell with the square fiber, while the response of the unit cell with the hexagonal fiber lies just above that of the unit cell with the circular fiber for both loading directions.

The effects of fiber shape on the transverse response of the unidirectional boron/aluminum composite illustrated herein are consistent with those reported by previous investigators that were recently summarized by Arnold, et al. (1996). In particular, the effect of fiber shape at low fiber volume fractions is small and increases with increasing fiber content. Square fibers provide the stiffest overall response (when the matrix strain hardens) and the highest flow stress (when the matrix does not strain harden) while circular fibers provide the most compliant response and the lowest flow stress. This is due to the square fiber's ability to provide a higher magnitude of hydrostatic stress in the matrix phase relative to the circular fiber, thereby delaying localized yielding and providing constraint on the expansion of the plastic zone throughout the matrix phase. Hexagonal fibers generate an intermediate response. It must be mentioned that the results reported in the literature addressing the effect of fiber shape on the response of MMCs are typically limited in scope, with a limited number of fiber shapes and typically a single strain hardening rate for the matrix phase. This is due to the computationally intensive finite-element approach typically employed to investigate these effects. Alternatively, the results generated with the reformulated version of the generalized method of cells that have been presented herein provide for the first time an exhaustive comparison of the fiber shape impact on the MMCs' transverse response as a function of the fiber volume fraction and the matrix phase's strain hardening capability. Similarly, the influence of the fiber arrangement on the response of MMCs, which has a reportedly greater impact than the fiber shape, can now be efficiently investigated.

The last set of results addresses the important question of the extent to which a given fiber shape should be approximated (the discretization level of the repeating unit cell) in order to obtain sufficiently accurate results for that shape. In particular, we consider increasing levels of cell discretization for a circular fiber to determine the level of microstructural refinement at which convergence to the "true" solution obtained from a highly discretized unit cell is achieved. The "true" solution is based on the previously employed unit cell containing a highly refined circular fiber shape generated using 120×120 subcells. The unit cells employed in this convergence study are shown in Fig. 8. In addition to the unit cells with the square fiber and the highly refined circular fiber, unit cells with a fiber in the shape of a cross containing 6×6 subcells and circular fibers approximated by 8×8 and 18×18 subcells were considered. The results for the transverse response of these unit cells containing the previously employed boron fiber and aluminum matrix are presented in Fig. 9 based on a fiber volume fraction of 0.40 and no strain hardening of the aluminum matrix. As observed previously, the response of the unit cell containing the highly refined circular fiber cannot be approximated in the plastic region by that containing the square fiber at this fiber volume fraction. Despite the fact that the elastic responses are virtually the same, the substantial strain hardening produced by the square fiber leads to the macroscopic flow stress for the composite which is more than 50% greater than that due to the circular fiber. The cross-shaped fiber produces a flow stress which is 20% higher than that due to the highly refined circular fiber. This difference reduces to 10% and 5% for the circular fibers approximated by 8×8 and 18×18 subcells, respectively.

CONCLUSIONS AND FUTURE PERSPECTIVES

The efficient implementation of the generalized method of cells outlined herein greatly facilitates analysis of unidirectional composites whose microstructures require a highly detailed geometric representation. This was accomplished by first reformulating the displacement continuity equations in the original formulation of the generalized method of cells in terms of subcell stress components and then directly incorporating the traction continuity conditions into these equations. This effectively replaces the subcell strains by the subcell interfacial tractions as the basic unknown microvariables, which in turn substantially reduces the size of the system of equations for the determination of these microvariables. This substantial reduction in the size of the system of equations for the unknown microvariables makes possible the inelastic analysis of repeating unit cells containing thousands of subcells which could not be analyzed previously. Consequently, repeating unit cells with highly detailed fiber shapes can now be analyzed efficiently in the presence of matrix plasticity as demonstrated herein. Comparison of CPU times required by the original and reformulated versions of the generalized method of cells to simulate the thermal heat-up response of a SiC/TiAl composite with temperature-dependent thermoelastoplastic constituent properties demonstrated a dramatic reduction in the execution times as a function of the number of subcells in the repeating unit cell due to the reformulation. Further, while the thermal analysis of repeating unit cells containing more than 100 subcells proved to be impractical using the original formulation, such analysis was perfomed efficiently using the new formulation in a fraction of the time required of the original formulation. This opens up the possibility of using the new formulation in conjunction with large-scale structural analyses to investigate the response of composite structures with microstructures that require detailed geometrical representations.

The examples presented herein were limited to the analysis of the transverse response of unidirectional metal matrix composites with highly refined elliptical, circular, diamond, and hexagonal fibers. The effect of the fiber cross section on the transverse response predicted by the reformulated generalized method of cells was consistent with the results reported in the literature. An additional study into the effect of different levels of circular fiber shape approximation on the transverse response of a undirectional composite revealed that a unit cell discretized into 18×18 subcells closely approximated the response obtained with a 120×120 subcell unit cell. The utility of the reformulated generalized method of cells, however, should become even more apparent when investigating the response of unidirectional composites with more than one type of fiber and with different fiber arrangements or arrays. The impact of the fiber array architecture on composite response is known to be substantially greater than that of the fiber shape. However, the impact of multi-phase fibers on composite response remains to be fully characterized. This can now easily be performed using the reformulated generalized method of cells. In addition, modeling of mechanisms that require detailed cell discretization, such as progressive damage accummulation due to crack growth or progressive interfacial debonding can also be efficiently realized.

The outlined reformulation of the generalized method of cells in terms of subcell interfacial tractions is expected to result in an even greater computational capability enhancement when applied to the three-dimensional version of the generalized method of cells developed by Aboudi (1995) for modeling

the response of inelastic multi-phase, short-fiber composites. This version has been employed by Herakovich and Baxter (1997) to investigate the effect of pore geometry on the inelastic response of porous media. The three-dimensional generalized method of cells has also been employed to model the mechanical response of woven graphite/copper composites by Bednarcyk, et al. (1997) using an embedded micromechanics-within-micromechanics model approach. In this approach, the instantaneous response of the individual fiber yarns, which occupy specified subcells in the three-dimensional representation of the woven composite, is determined at each point along the loading path using the original method of cells (Aboudi, 1991) and then subsequently used in the global three-dimensional generalized method of cells analysis. However, the three-dimensional discretization of the repeating unit cell substantially increases the number of unknown microvariables that must be determined, thereby placing a limit on the level of microstructural refinement of the weave geometry. In order to be able to model three-dimensional woven composites using a sufficiently detailed representation of the weave geometry, the three-dimensional generalized method of cells has recently been reformulated along similar lines presented herein for the two-dimensional version. The details of this reformulation and the comparison of the analytical predictions with experimental data will be reported in the future.

Finally, the reformulation of the displacement continuity equations in terms of the interfacial subcell tractions as the unknown microvariables produces a system of equations characterized by a matrix that consists of two diagonal submatrices and two fully-populated off-diagonal submatrices in the case of the two-dimensional generalized method of cells. In the case of the three-dimensional generalized method of cells, on the other hand, the matrix consists of thirty-six submatrices of which only twelve are fully-populated. Therefore, further computational efficiency enhancement can be accomplished for both versions of the generalized method of cells through Orozco's sparse implementation approach.

ACKNOWLEDGEMENTS

The authors gratefully acknowledge the support provided by the NASA-Lewis Research Center through the grants **NAG3-1377** and **NAG3-1319**. In particular, the authors are indebted to Dr. Steven M. Arnold, Dr. Robert V. Miner, Dr. David Ellis and Dr. Michael V. Nathal for their continuous support and assistance throughout this investigation.

REFERENCES

Aboudi, J. (1991), *Mechanics of Composite Materials: A Unified Micromechanical Approach*, Elsevier, The Netherlands.

Aboudi, J. (1993), "Constitutive Behavior of Multiphase Metal Matrix Composites with Interfacial Damage by the Generalized Cell Model," in *Damage in Composite Materials*, G. Z. Voyiadjis (Ed.), pp. 3-22. Elsevier, Amsterdam.

Aboudi, J. (1995), "Micromechanical Analysis of Thermo-Inelastic Multiphase Short-Fiber Composites," *Composites Engineering*, Vol. 5, No. 7, pp. 839-850.

Arnold, S. M., Pindera, M-J., and Wilt, T. E. (1996), "Influence of Fiber Architecture on the Inelastic Response of Metal Matrix Composites," *Int. Journal of Plasticity*, Vol. 12, No. 4, pp. 507-545.

Bednarcyk, B. A., Pauly, C. C., and Pindera, M-J. (1997), "Experimental Characterization and Micromechanical Modeling of Woven Carbon/Copper Composites," *NASA Contractor Report 202318*, Lewis Research Center, Cleveland, OH.

Herakovich, C. T. and Baxter, S. C. (1997), "Influence of Pore Geometry on the Inelastic Response of Porous Media," (in preparation).

Hill, R. (1963), "Elastic Properties of Reinforced Solids: Some Theoretical Principles," *J. Mech. Phys. Solids*, Vol. 11, pp. 357-372.

Mendelson, A. (1983), *Plasticity: Theory and Applications*, Robert E. Krieger Publishing Company, Malabar, FL., (reprint edition).

Orozco, C. E. (1997), "Computational Aspects of Modeling Complex Microstructure Composites Using GMC," *Composites Part B*, Vol. 28B, No. 1/2, pp. 167-175.

Paley, M. and Aboudi, J. (1992), "Micromechanical Analysis of Composites by the Generalized Cells Model," *Mechanics of Materials*, Vol. 14, pp. 127-139.

Williams, T. O. and Pindera, M-J. (1997), "An Analytical Model for the Inelastic Axial Shear Response of Unidirectional Metal Matrix Composites," *Int. Journal of Plasticity* (in press).

APPENDIX

Relations between subcell normal tractions and macroscopic normal strains

To develop the relations between subcell normal tractions and macroscopic normal strains, we first express the subcell normal strains in terms of the subcell normal stresses, and plastic and thermal strains using eqn (25).

$$\bar{\varepsilon}_{11}^{(\beta\gamma)} = S_{11}^{(\beta\gamma)}\bar{\sigma}_{11}^{(\beta\gamma)} + S_{12}^{(\beta\gamma)}\bar{\sigma}_{22}^{(\beta\gamma)} + S_{13}^{(\beta\gamma)}\bar{\sigma}_{33}^{(\beta\gamma)} + \alpha_{11}^{(\beta\gamma)}\Delta T + \bar{\varepsilon}_{11}^{p(\beta\gamma)} \tag{A1}$$

$$\bar{\varepsilon}_{22}^{(\beta\gamma)} = S_{12}^{(\beta\gamma)}\bar{\sigma}_{11}^{(\beta\gamma)} + S_{22}^{(\beta\gamma)}\bar{\sigma}_{22}^{(\beta\gamma)} + S_{23}^{(\beta\gamma)}\bar{\sigma}_{33}^{(\beta\gamma)} + \alpha_{22}^{(\beta\gamma)}\Delta T + \bar{\varepsilon}_{22}^{p(\beta\gamma)} \tag{A2}$$

$$\bar{\varepsilon}_{33}^{(\beta\gamma)} = S_{13}^{(\beta\gamma)}\bar{\sigma}_{11}^{(\beta\gamma)} + S_{23}^{(\beta\gamma)}\bar{\sigma}_{22}^{(\beta\gamma)} + S_{33}^{(\beta\gamma)}\bar{\sigma}_{33}^{(\beta\gamma)} + \alpha_{33}^{(\beta\gamma)}\Delta T + \bar{\varepsilon}_{33}^{p(\beta\gamma)} \tag{A3}$$

Using the constraint on the axial deformation in all subcells, $\bar{\varepsilon}_{11}^{(\beta\gamma)} = \bar{\varepsilon}_{11}$, in eqn (A1), the axial subcell stress $\bar{\sigma}_{11}^{(\beta\gamma)}$ is expressed as follows,

$$\bar{\sigma}_{11}^{(\beta\gamma)} = \frac{1}{S_{11}^{(\beta\gamma)}}[\bar{\varepsilon}_{11} - \alpha_{11}^{(\beta\gamma)}\Delta T - \bar{\varepsilon}_{11}^{p(\beta\gamma)} - S_{12}^{(\beta\gamma)}\bar{\sigma}_{22}^{(\beta\gamma)} - S_{13}^{(\beta\gamma)}\bar{\sigma}_{33}^{(\beta\gamma)}] \tag{A4}$$

The above expression is then used in eqns (A2) and (A3) to eliminate the axial subcell stress $\bar{\sigma}_{11}^{(\beta\gamma)}$ from the expressions for the subcell normal strains $\bar{\varepsilon}_{22}^{(\beta\gamma)}$ and $\bar{\varepsilon}_{33}^{(\beta\gamma)}$,

$$\bar{\varepsilon}_{22}^{(\beta\gamma)} = \frac{S_{12}^{(\beta\gamma)}}{S_{11}^{(\beta\gamma)}}\bar{\varepsilon}_{11} + (S_{22}^{(\beta\gamma)} - \frac{S_{12}^{(\beta\gamma)^2}}{S_{11}^{(\beta\gamma)}})\bar{\sigma}_{22}^{(\beta\gamma)} + (S_{23}^{(\beta\gamma)} - \frac{S_{12}^{(\beta\gamma)}S_{13}^{(\beta\gamma)}}{S_{11}^{(\beta\gamma)}})\bar{\sigma}_{33}^{(\beta\gamma)} + (\alpha_{22}^{(\beta\gamma)} - \frac{S_{12}^{(\beta\gamma)}}{S_{11}^{(\beta\gamma)}}\alpha_{11}^{(\beta\gamma)})\Delta T +$$

$$\bar{\varepsilon}_{22}^{p(\beta\gamma)} - \frac{S_{12}^{(\beta\gamma)}}{S_{11}^{(\beta\gamma)}}\bar{\varepsilon}_{11}^{p(\beta\gamma)} \tag{A5}$$

$$\bar{\varepsilon}_{33}^{(\beta\gamma)} = \frac{S_{13}^{(\beta\gamma)}}{S_{11}^{(\beta\gamma)}}\bar{\varepsilon}_{11} + (S_{23}^{(\beta\gamma)} - \frac{S_{12}^{(\beta\gamma)}S_{13}^{(\beta\gamma)}}{S_{11}^{(\beta\gamma)}})\bar{\sigma}_{22}^{(\beta\gamma)} + (S_{33}^{(\beta\gamma)} - \frac{S_{13}^{(\beta\gamma)^2}}{S_{11}^{(\beta\gamma)}})\bar{\sigma}_{33}^{(\beta\gamma)} + (\alpha_{33}^{(\beta\gamma)} - \frac{S_{13}^{(\beta\gamma)}}{S_{11}^{(\beta\gamma)}}\alpha_{11}^{(\beta\gamma)})\Delta T +$$

$$\bar{\varepsilon}_{33}^{p(\beta\gamma)} - \frac{S_{13}^{(\beta\gamma)}}{S_{11}^{(\beta\gamma)}}\bar{\varepsilon}_{11}^{p(\beta\gamma)} \tag{A6}$$

Equations (A5) and (A6) are subsequently used in the interfacial displacement continuity conditions (12b) and (12d) in order to express them in terms of the normal subcell stresses $\bar{\sigma}_{22}^{(\beta\gamma)}$ and $\bar{\sigma}_{33}^{(\beta\gamma)}$,

$$\sum_{\beta=1}^{N_\beta} h_\beta (S_{22}^{(\beta\gamma)} - \frac{S_{12}^{(\beta\gamma)^2}}{S_{11}^{(\beta\gamma)}}) \bar{\sigma}_{22}^{(\beta\gamma)} + \sum_{\beta=1}^{N_\beta} h_\beta (S_{23}^{(\beta\gamma)} - \frac{S_{12}^{(\beta\gamma)} S_{13}^{(\beta\gamma)}}{S_{11}^{(\beta\gamma)}}) \bar{\sigma}_{33}^{(\beta\gamma)} = h\bar{\varepsilon}_{22} - (\sum_{\beta=1}^{N_\beta} h_\beta \frac{S_{12}^{(\beta\gamma)}}{S_{11}^{(\beta\gamma)}}) \bar{\varepsilon}_{11} +$$

$$\sum_{\beta=1}^{N_\beta} h_\beta (\frac{S_{12}^{(\beta\gamma)}}{S_{11}^{(\beta\gamma)}} \alpha_{11}^{(\beta\gamma)} - \alpha_{22}^{(\beta\gamma)}) \Delta T + \sum_{\beta=1}^{N_\beta} h_\beta (\frac{S_{12}^{(\beta\gamma)}}{S_{11}^{(\beta\gamma)}} \bar{\varepsilon}_{11}^{p(\beta\gamma)} - \bar{\varepsilon}_{22}^{p(\beta\gamma)}), \quad \gamma = 1,..., N_\gamma \tag{A7}$$

$$\sum_{\gamma=1}^{N_\gamma} l_\gamma (S_{23}^{(\beta\gamma)} - \frac{S_{12}^{(\beta\gamma)} S_{13}^{(\beta\gamma)}}{S_{11}^{(\beta\gamma)}}) \bar{\sigma}_{22}^{(\beta\gamma)} + \sum_{\gamma=1}^{N_\gamma} l_\gamma (S_{33}^{(\beta\gamma)} - \frac{S_{13}^{(\beta\gamma)^2}}{S_{11}^{(\beta\gamma)}}) \bar{\sigma}_{33}^{(\beta\gamma)} = l\bar{\varepsilon}_{33} - (\sum_{\gamma=1}^{N_\gamma} l_\gamma \frac{S_{13}^{(\beta\gamma)}}{S_{11}^{(\beta\gamma)}}) \bar{\varepsilon}_{11} +$$

$$\sum_{\gamma=1}^{N_\gamma} l_\gamma (\frac{S_{13}^{(\beta\gamma)}}{S_{11}^{(\beta\gamma)}} \alpha_{11}^{(\beta\gamma)} - \alpha_{33}^{(\beta\gamma)}) \Delta T + \sum_{\gamma=1}^{N_\gamma} l_\gamma (\frac{S_{13}^{(\beta\gamma)}}{S_{11}^{(\beta\gamma)}} \bar{\varepsilon}_{11}^{p(\beta\gamma)} - \bar{\varepsilon}_{33}^{p(\beta\gamma)}), \quad \beta = 1,..., N_\beta \tag{A8}$$

Use of the interfacial traction continuity conditions (26) and (27) in the above expresions yields eqns (28) and (29).

Relations between subcell shear tractions and macroscopic shear strains

To develop the relations between subcell shear tractions and macroscopic shear strains, we first express the subcell shear strains in terms of the subcell shear stresses, and plastic and thermal strains using eqn (25).

$$\bar{\varepsilon}_{12}^{(\beta\gamma)} = \frac{1}{2} S_{66}^{(\beta\gamma)} \bar{\sigma}_{12}^{(\beta\gamma)} + \bar{\varepsilon}_{12}^{p(\beta\gamma)}, \quad \bar{\varepsilon}_{13}^{(\beta\gamma)} = \frac{1}{2} S_{55}^{(\beta\gamma)} \bar{\sigma}_{13}^{(\beta\gamma)} + \bar{\varepsilon}_{13}^{p(\beta\gamma)}, \quad \bar{\varepsilon}_{23}^{(\beta\gamma)} = \frac{1}{2} S_{44}^{(\beta\gamma)} \bar{\sigma}_{23}^{(\beta\gamma)} + \bar{\varepsilon}_{23}^{p(\beta\gamma)} \tag{A9)-(A11}$$

Equations (A9) through (A11) are subsequently used in the interfacial displacement continuity conditions (12c), (12e) and (12f) in order to express them in terms of the subcell shear stresses $\bar{\sigma}_{12}^{(\beta\gamma)}$, $\bar{\sigma}_{13}^{(\beta\gamma)}$, and $\bar{\sigma}_{23}^{(\beta\gamma)}$,

$$\frac{1}{2} \sum_{\beta=1}^{N_\beta} h_\beta S_{66}^{(\beta\gamma)} \bar{\sigma}_{12}^{(\beta\gamma)} = h\bar{\varepsilon}_{12} - \sum_{\beta=1}^{N_\beta} h_\beta \bar{\varepsilon}_{12}^{p(\beta\gamma)}, \quad \gamma = 1,..., N_\gamma \tag{A12}$$

$$\frac{1}{2} \sum_{\gamma=1}^{N_\gamma} l_\gamma S_{55}^{(\beta\gamma)} \bar{\sigma}_{13}^{(\beta\gamma)} = l\bar{\varepsilon}_{13} - \sum_{\gamma=1}^{N_\gamma} l_\gamma \bar{\varepsilon}_{13}^{p(\beta\gamma)}, \quad \beta = 1,..., N_\beta \tag{A13}$$

$$\frac{1}{2} \sum_{\beta=1}^{N_\beta} \sum_{\gamma=1}^{N_\gamma} h_\beta l_\gamma S_{44}^{(\beta\gamma)} \bar{\sigma}_{23}^{(\beta\gamma)} = hl\bar{\varepsilon}_{23} - \sum_{\beta=1}^{N_\beta} \sum_{\gamma=1}^{N_\gamma} h_\beta l_\gamma \bar{\varepsilon}_{23}^{p(\beta\gamma)} \tag{A14}$$

Use of the interfacial traction continuity conditions (32), (33), (36) and (37) in the above expresions yields eqns (34), (35) and (38).

Table 1. Material properties of SiC fiber and titanium aluminide matrix.

Material properties	24 °C	200 °C	425 °C	600 °C	650 °C	815 °C
SiC fiber						
α (x 10^{-6} cm/cm/ °C)	3.53	3.62	3.87	4.19	4.28	4.5
Young's modulus (GPa)	400.0	400.0	400.0	400.0	400.0	400.0
Poisson's ratio	0.25	0.25	0.25	0.25	0.25	0.25
Ti-24Al-11Nb matrix						
α (x 10^{-6} cm/cm/ °C)	9.0	9.36	10.26	10.53	10.62	11.07
Young's modulus (GPa)	110.3	100.0	75.8	86.2	68.2	11.2
Poisson's ratio	0.26	0.26	0.26	0.26	0.26	0.26
Yield stress (MPa)	371.5	406.7	370.2	290.9	269.5	165.5
Hardening slope (GPa)	22.98	3.04	2.22	1.29	0.67	0.00

Table 2. Comparison of CPU times required by the original and reformulated versions of the generalized method of cells to generate a thermal heat-up response of a SiC/TiAl unidirectional composite.

GMC version	CPU times (seconds) as a function of the number of subcells							
	2x2	4x4	6x6	8x8	10x10	12x12	20x20	100x100
original	0.87	19	182	508	8,679	43,781	-	-
reformulated	0.18	0.25	0.5	0.9	1.5	2.3	8.3	796

Table 3. Material properties of the boron fiber and aluminum matrix.

Material	Young's modulus (GPa)	Poisson's ratio	Hardening slope (GPa)
Boron fiber	414.0	0.20	N/A
Aluminum matrix	55.2	0.30	E/10,000 and E/5

Note: The hardening slope is the secondary slope in a bilinear stress-strain representation of the matrix phase's elastic-plastic response.

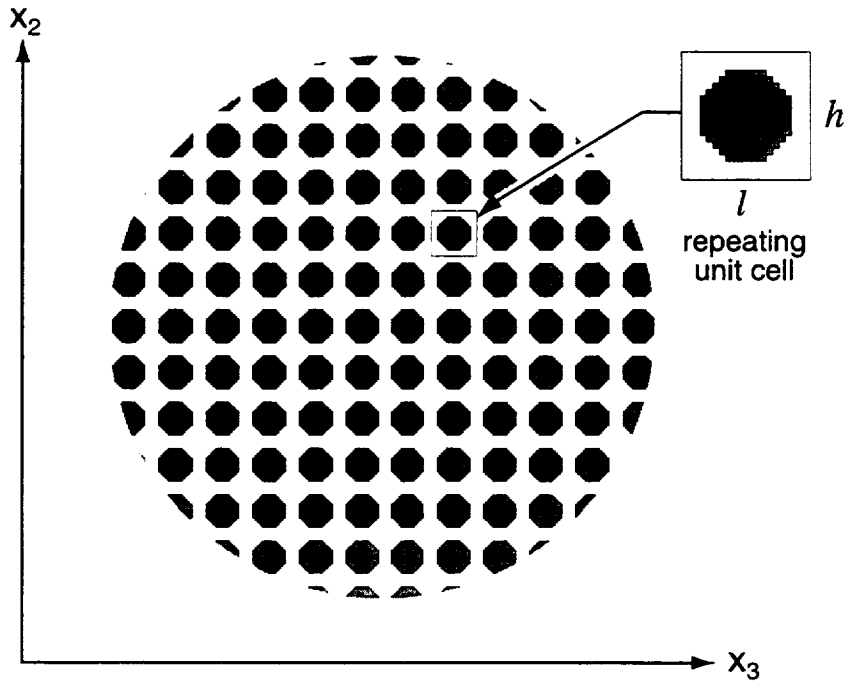

Doubly periodic array of fibers

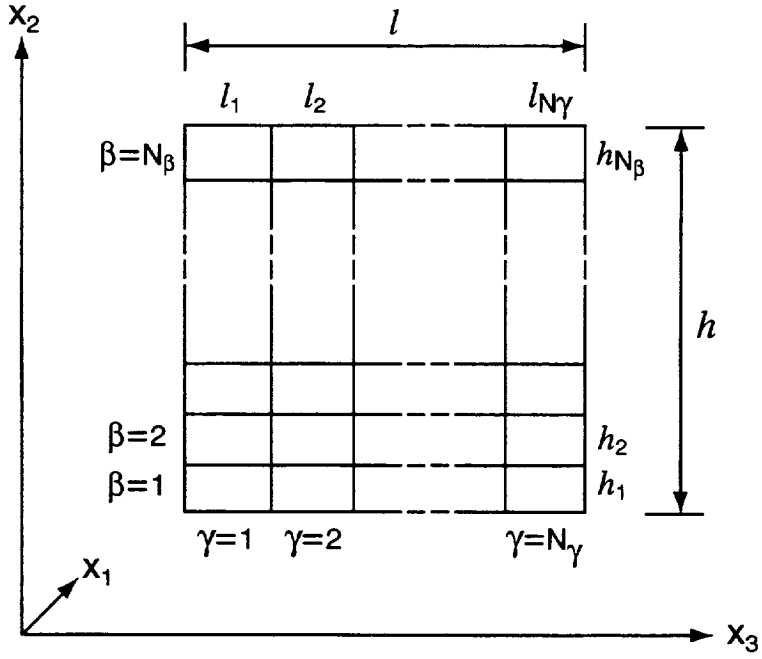

Discretization of the repeating unit cell

Figure 1. A unidirectional composite modeled by the generalized method of cells as a doubly-periodic array of fibers (top), and the details of the repeating unit cell discretization (bottom).

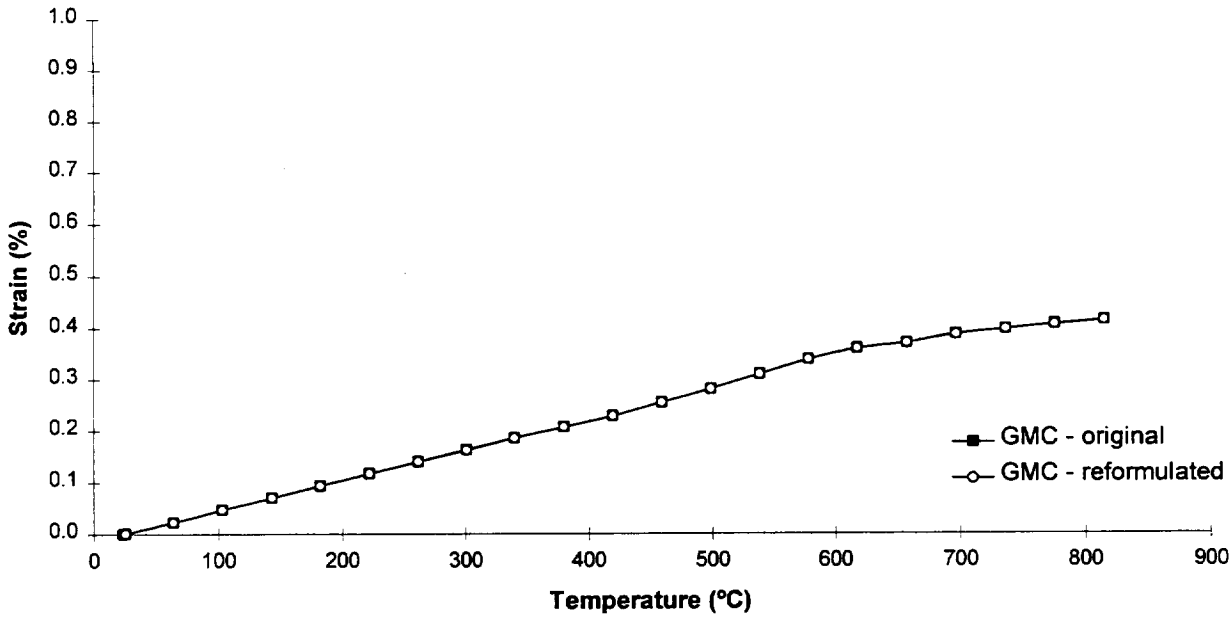

(a)

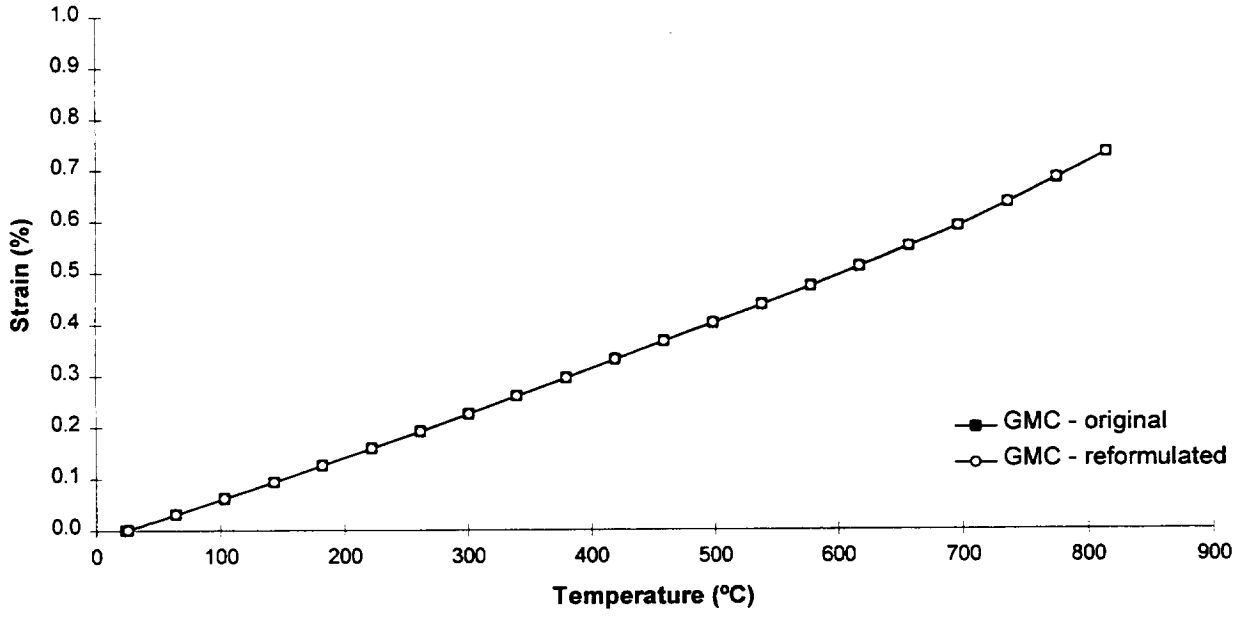

(b)

Figure 2. Thermal response of a unidirectional SiC/TiAl composite predicted by the original and reformulated versions of the generalized method of cells: (a) longitudinal; (b) transverse.

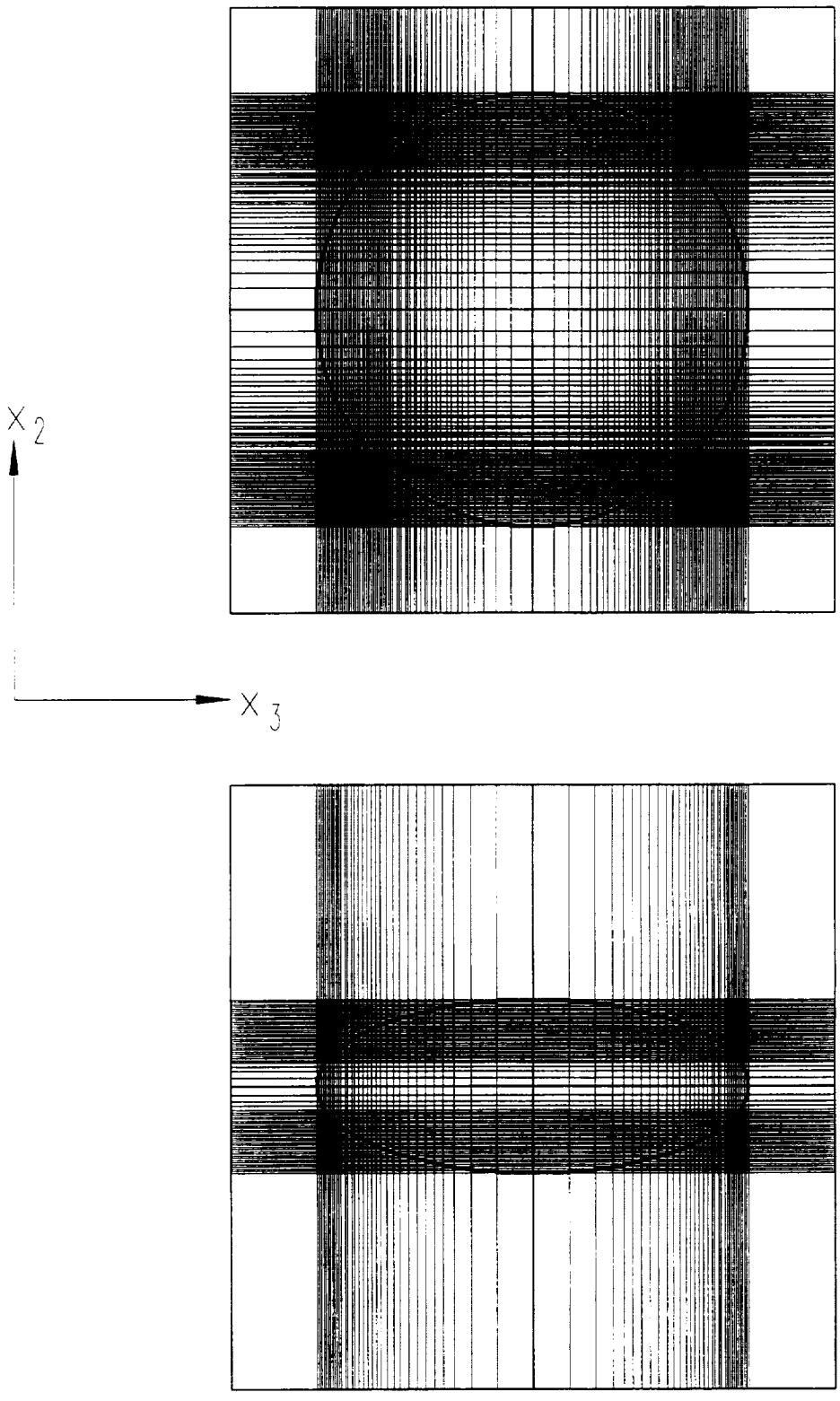

Figure 3. Repeating unit cells with circular and elliptical fibers discretized into 120×120 and 68×68 subcells, respectively.

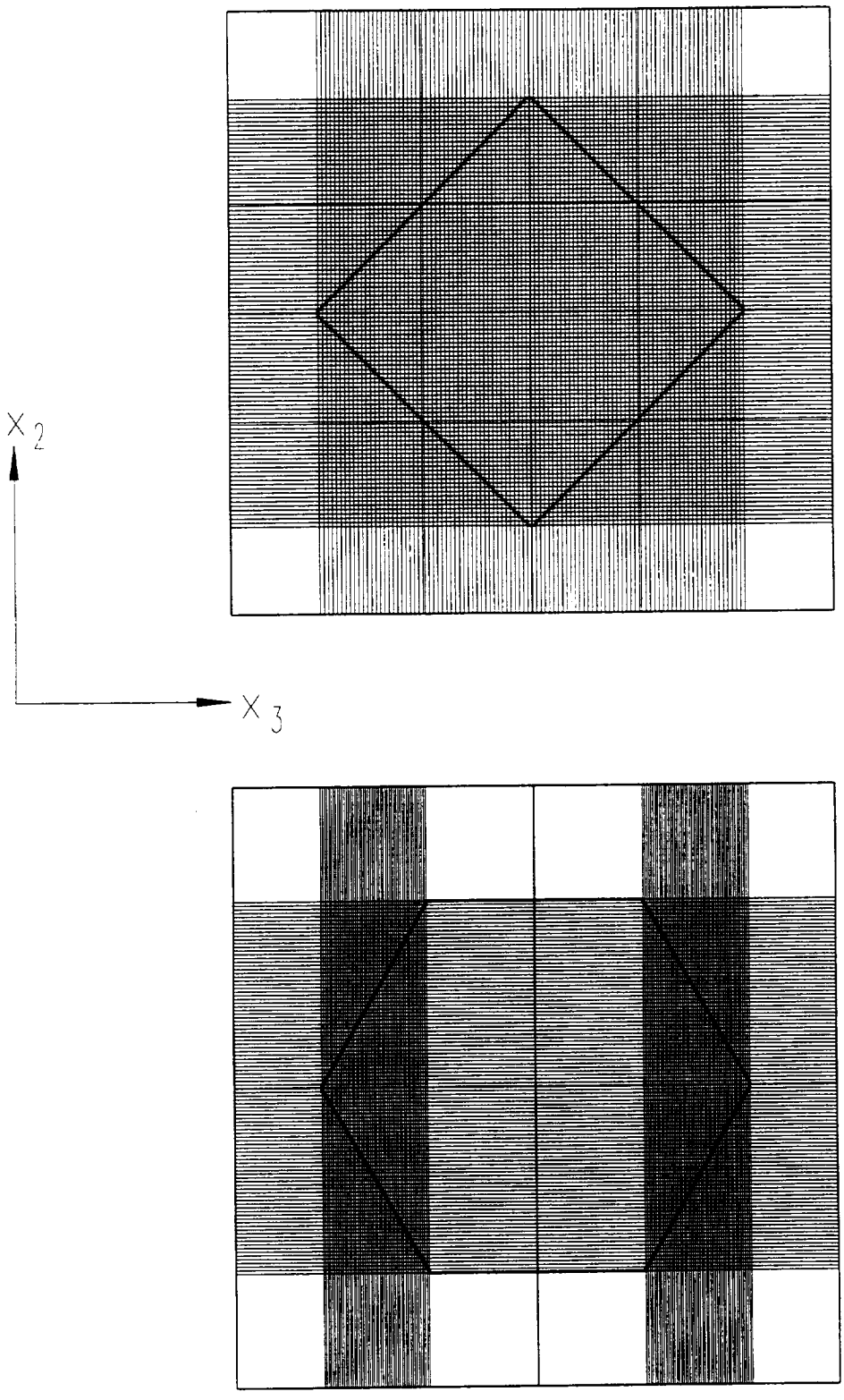

Figure 3 (cont'd). Repeating unit cells with diamond and hexagonal fibers discretized into 102×102 subcells.

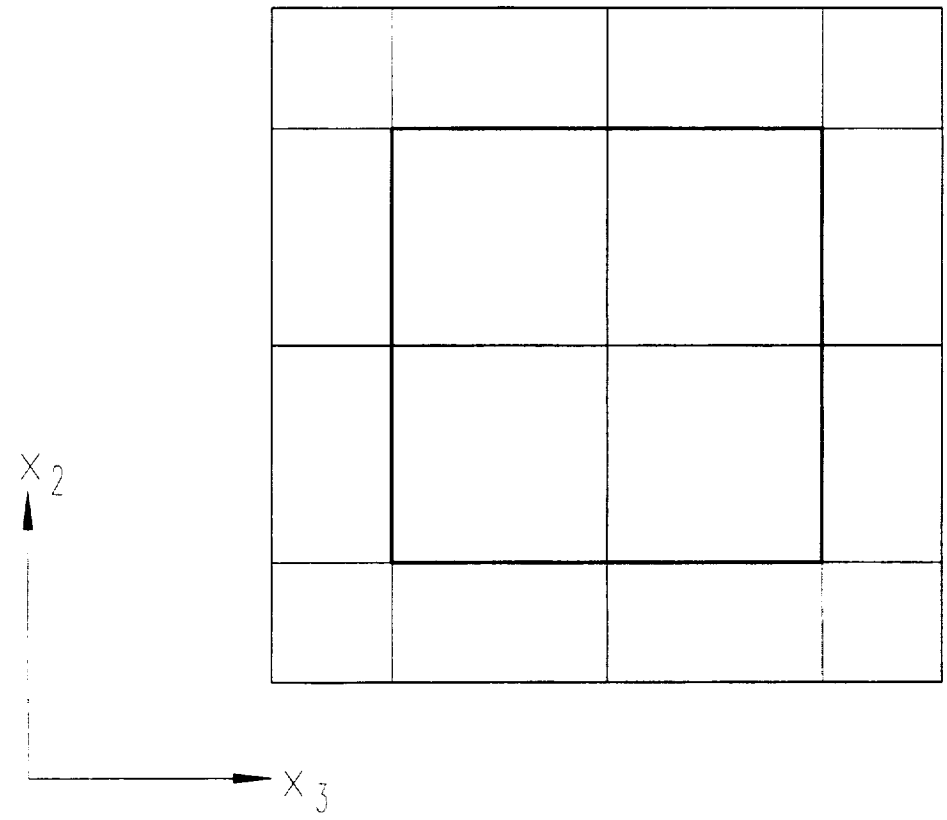

Figure 3 (cont'd). Repeating unit cell with a square fiber discretized into 4×4 subcells.

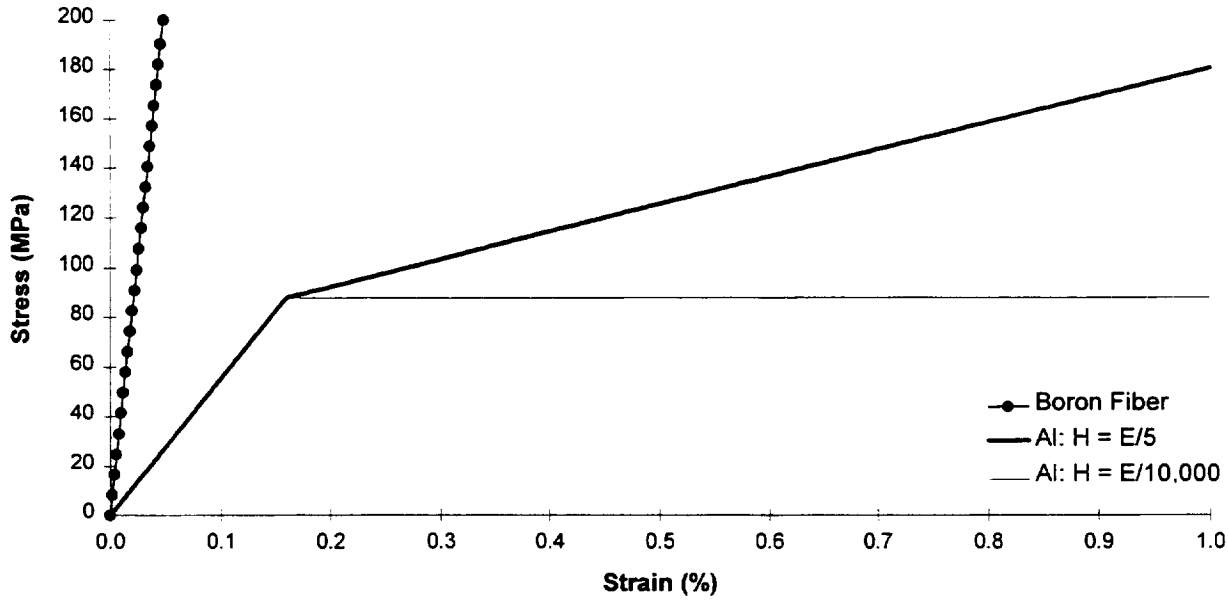

Figure 4. Stress-strain response of the constituent phases in the B/Al composite.

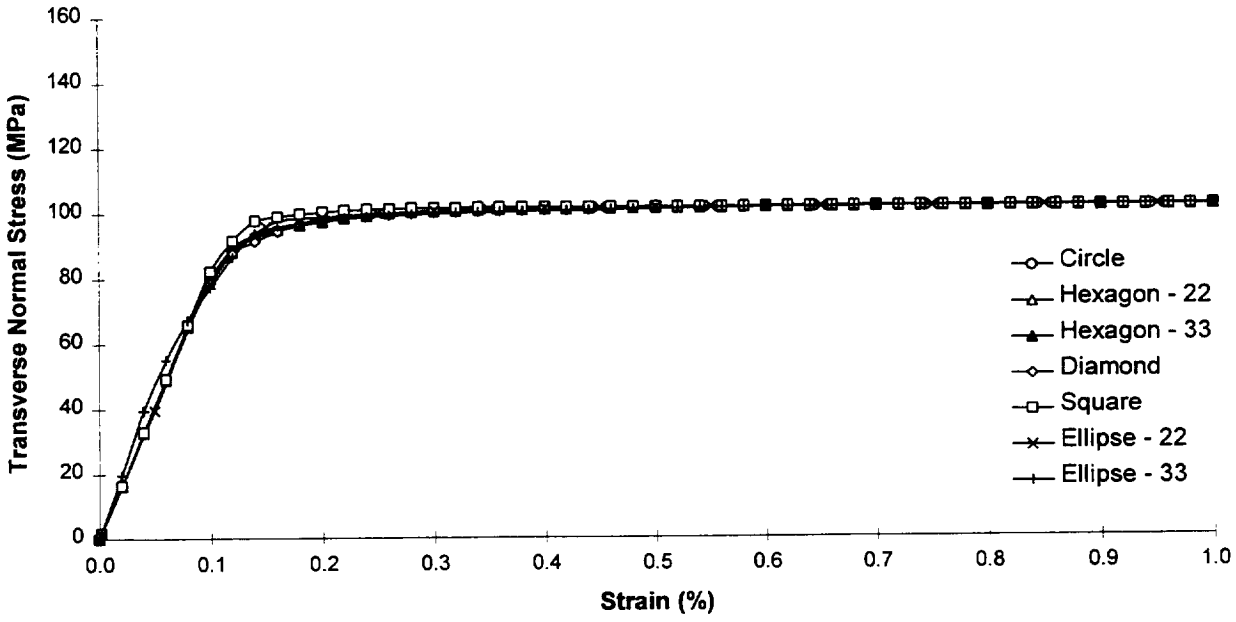

(a)

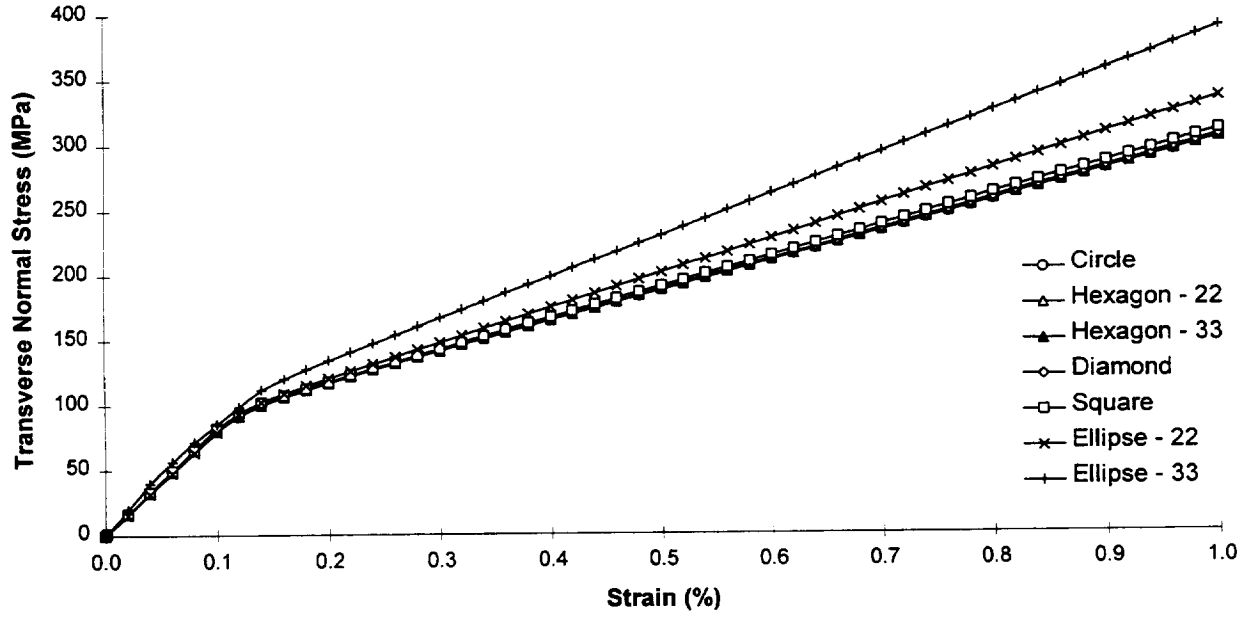

(b)

Figure 5. Transverse response of a unidirectional B/Al composite with differently-shaped fibers containing 0.25 fiber volume fraction: (a) H = E/10,000; (b) H = E/5.

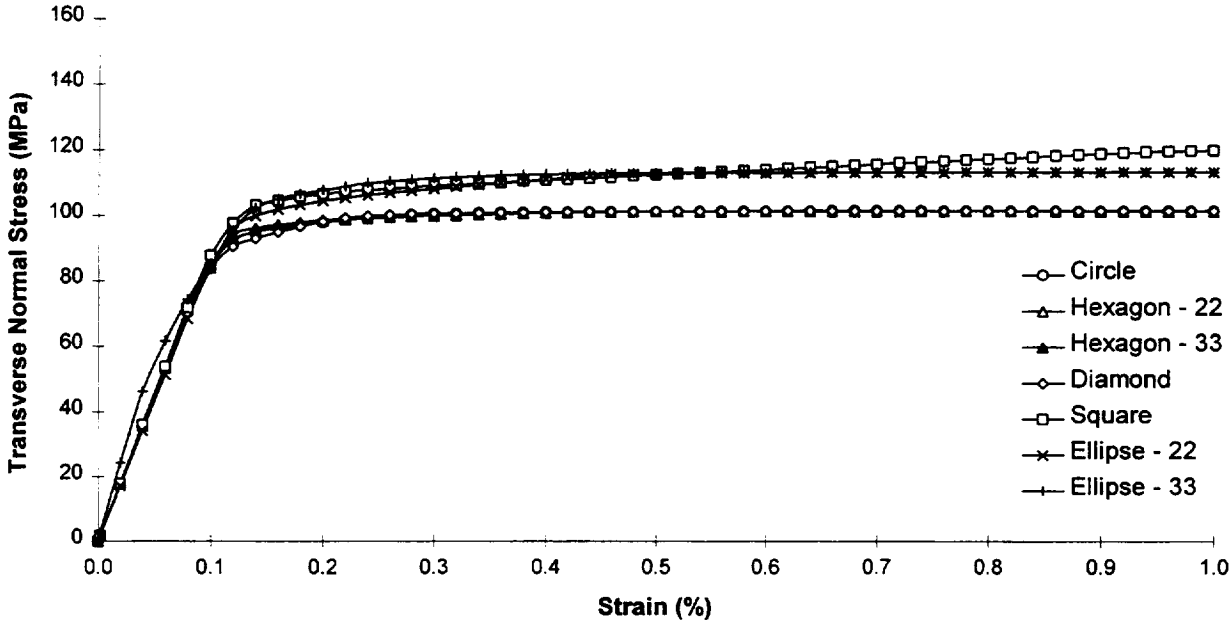

(a)

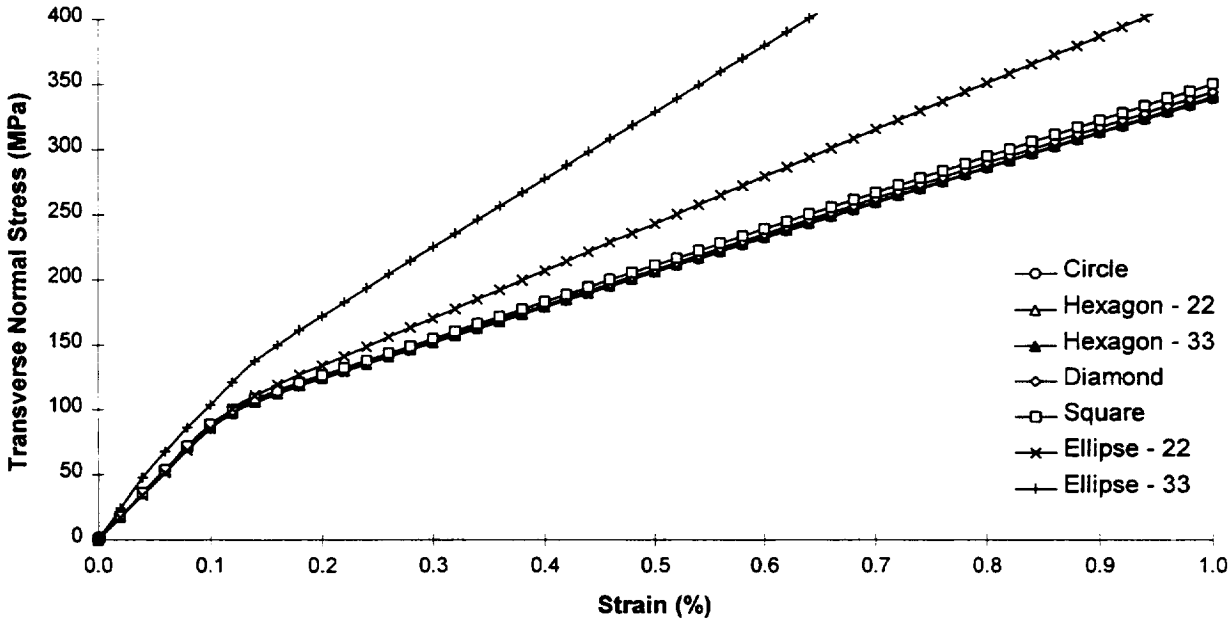

(b)

Figure 6. Transverse response of a unidirectional B/Al composite with differently-shaped fibers containing 0.30 fiber volume fraction: (a) H = E/10,000; (b) H = E/5.

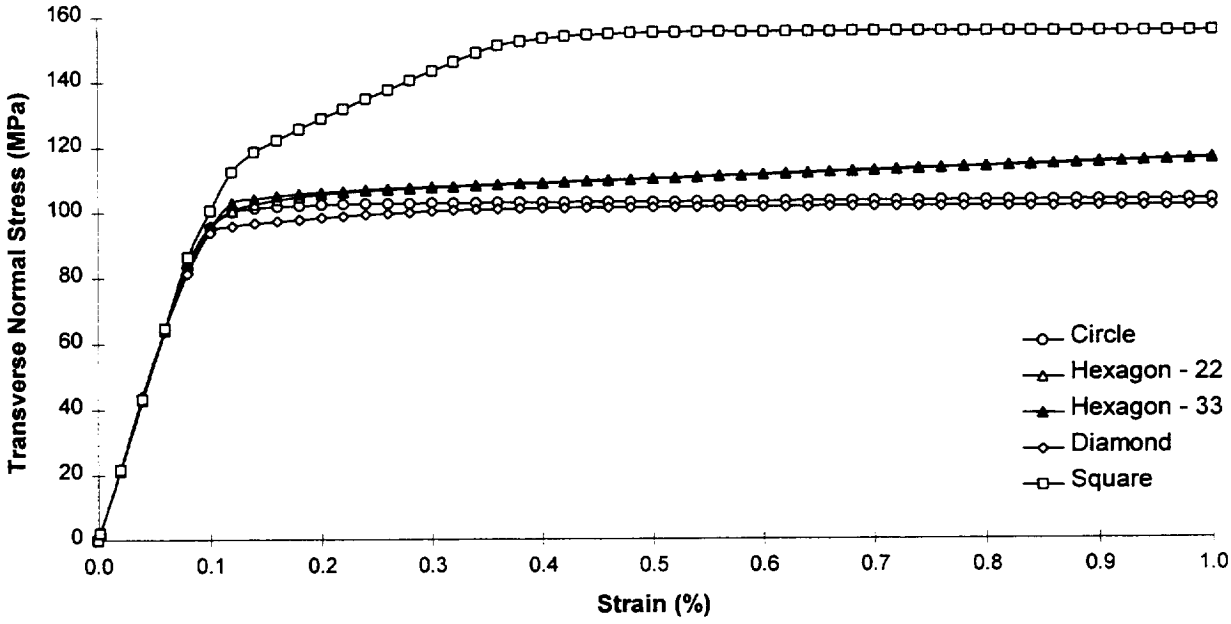

(a)

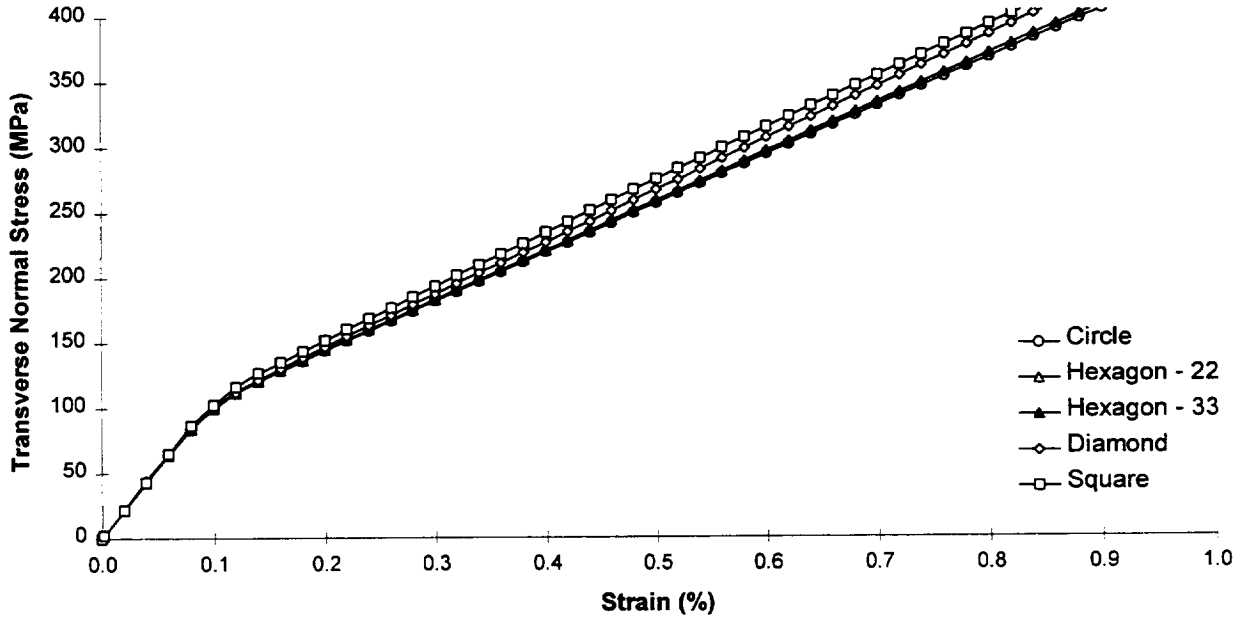

(b)

Figure 7. Transverse response of a unidirectional B/Al composite with differently-shaped fibers containing 0.40 fiber volume fraction: (a) H = E/10,000; (b) H = E/5.

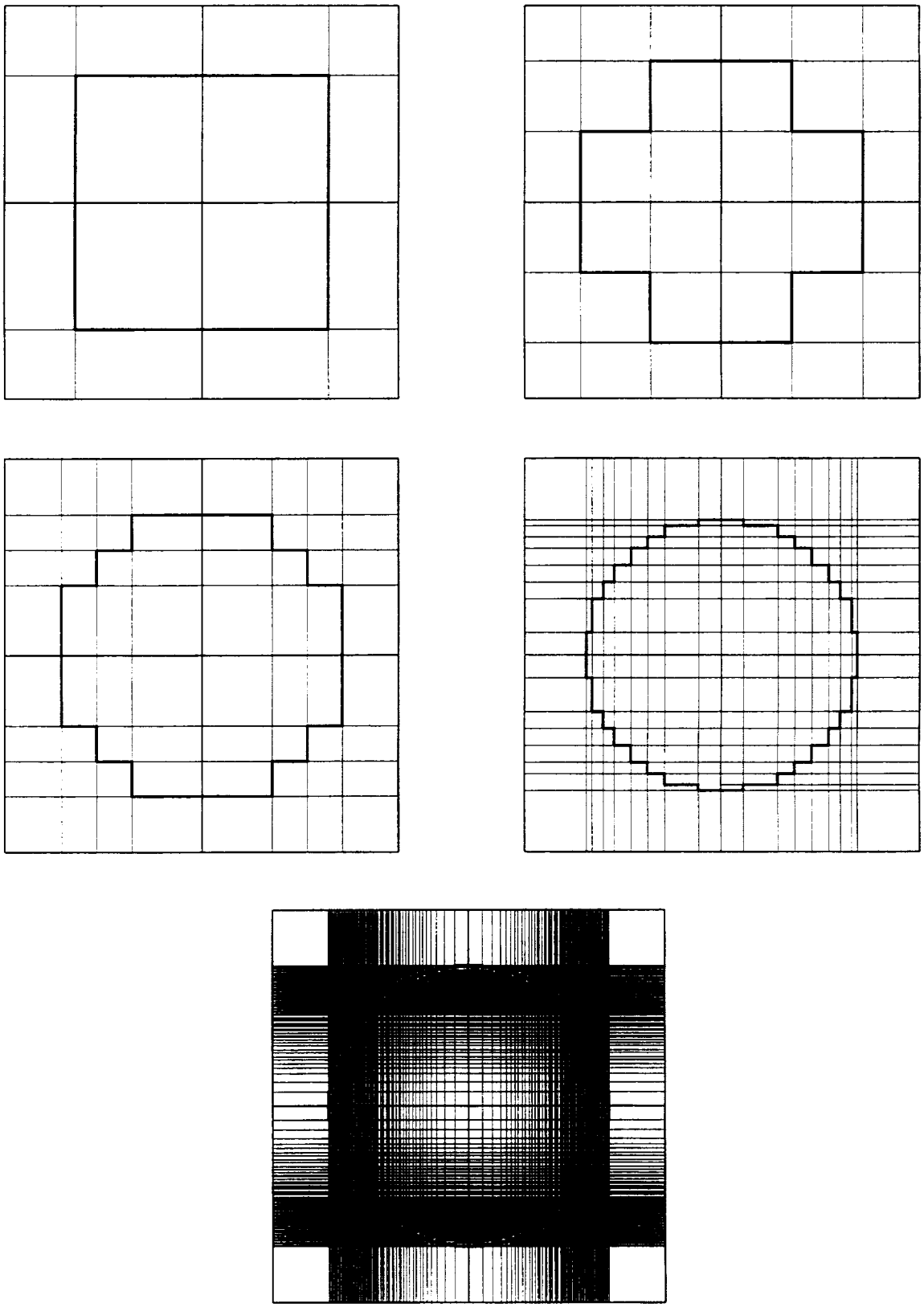

Figure 8. Repeating unit cells containing fibers with increasingly refined circular fiber shape.

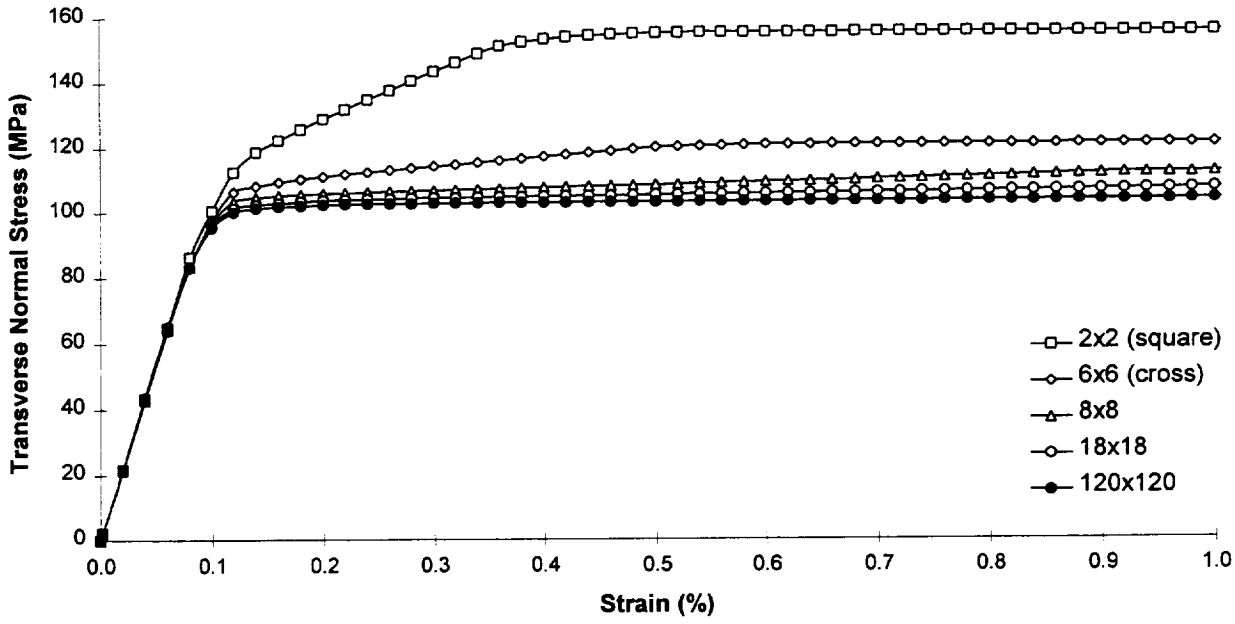

Figure 9. Transverse response of repeating unit cells containing fibers with increasingly refined circular fiber shape.

REPORT DOCUMENTATION PAGE

Form Approved
OMB No. 0704-0188

1. AGENCY USE ONLY (Leave blank)	2. REPORT DATE	3. REPORT TYPE AND DATES COVERED
	May 1997	Final Contractor Report

4. TITLE AND SUBTITLE

An Efficient Implementation of the GMC Micromechanics Model for Multi-Phased Materials With Complex Microstructures

5. FUNDING NUMBERS

WU–523–21–13
G–NAG3–1377
G–NAS3–1319

6. AUTHOR(S)

Marek-Jerzy Pindera and Brett A. Bednarcyk

7. PERFORMING ORGANIZATION NAME(S) AND ADDRESS(ES)

University of Virginia
Civil Engineering & Applied Mechanics Department
Charlottesville, Virginia 22903

8. PERFORMING ORGANIZATION REPORT NUMBER

E–10770

9. SPONSORING/MONITORING AGENCY NAME(S) AND ADDRESS(ES)

National Aeronautics and Space Administration
Lewis Research Center
Cleveland, Ohio 44135–3191

10. SPONSORING/MONITORING AGENCY REPORT NUMBER

NASA CR–202350

11. SUPPLEMENTARY NOTES

Project Manager, S.M. Arnold, Structures and Acoustics Division, NASA Lewis Research Center, organization code 5920, (216) 433–3334.

12a. DISTRIBUTION/AVAILABILITY STATEMENT

Unclassified - Unlimited
Subject Category 24

This publication is available from the NASA Center for AeroSpace Information, (301) 621–0390.

12b. DISTRIBUTION CODE

13. ABSTRACT ***(Maximum 200 words)***

An efficient implementation of the generalized method of cells micromechanics model is presented that allows analysis of periodic unidirectional composites characterized by repeating unit cells containing thousands of subcells. The original formulation, given in terms of Hill's strain concentration matrices that relate average subcell strains to the macroscopic strains, is reformulated in terms of the interfacial subcell tractions as the basic unknowns. This is accomplished by expressing the displacement continuity equations in terms of the stresses and then imposing the traction continuity conditions directly. The result is a mixed formulation wherein the unknown interfacial subcell traction components are related to the macroscopic strain components. Because the stress field throughout the repeating unit cell is piece-wise uniform, the imposition of traction continuity conditions directly in the displacement continuity equations, expressed in terms of stresses, substantially reduces the number of unknown subcell traction (and stress) components, and thus the size of the system of equations that must be solved. Further reduction in the size of the system of continuity equations is obtained by separating the normal and shear traction equations in those instances where the individual subcells are, at most, orthotropic. The reformulated version facilitates detailed analysis of the impact of the fiber cross-section geometry and arrangement on the response of multi-phased unidirectional composites with and without evolving damage. Comparison of execution times obtained with the original and reformulated versions of the generalized method of cells demonstrates the new version's efficiency.

14. SUBJECT TERMS	15. NUMBER OF PAGES
Micromechanics; Efficiency; Composites; Architecture; Deformation	35
	16. PRICE CODE: A03

17. SECURITY CLASSIFICATION OF REPORT	18. SECURITY CLASSIFICATION OF THIS PAGE	19. SECURITY CLASSIFICATION OF ABSTRACT	20. LIMITATION OF ABSTRACT
Unclassified	Unclassified	Unclassified	